

https://doi.org/10.11646/zootaxa.4577.3.1
http://zoobank.org/urn:lsid:zoobank.org:pub:1C7D3DF5-035D-44E2-AF8F-F732699D5C4B

Osteology and systematics of *Uberabatitan ribeiroi* (Dinosauria; Sauropoda): a Late Cretaceous titanosaur from Minas Gerais, Brazil

JULIAN C. G. SILVA JUNIOR^{1,2,5}, THIAGO S. MARINHO^{2,3},
AGUSTÍN G. MARTINELLI⁴ & MAX C. LANGER¹

¹Laboratorio de Paleontología de Ribeirão Preto, Faculdade de Filosofia, Ciências e Letras de Ribeirão Preto, Universidade de São Paulo, Av. Bandeirantes, 3900, 14040-901, Ribeirão Preto, São Paulo, Brazil.

E-mail: juliancristiangoncalves@gmail.com, mclanger@ffclrp.usp.br

²Centro de Pesquisas Paleontológicas “Llewelyn Ivor Price”, Universidade Federal do Triângulo Mineiro, Peirópolis, Estanislau Collenghi 194, 38039-755, Peirópolis, Uberaba, Minas Gerais, Brazil.

³Instituto de Ciências Exatas, Naturais e Educação, Universidade Federal do Triângulo Mineiro, Departamento de Ciências Biológicas, Av. Doutor Randolph Borges Júnior, 38064-200, Uberaba, Minas Gerais, Brazil. E-mail: thiago.marinho@uftm.edu.br

⁴CONICET-Sección Paleontología de Vertebrados, Museo Argentino de Ciencias Naturales ‘Bernardino Rivadavia’, Av. Ángel Galardo 470, Buenos Aires, C1405DJR, Argentina. E-mail: agustin_martinelli@yahoo.com.ar

⁵Corresponding author

Abstract

Uberabatitan ribeiroi is a Late Cretaceous titanosaur (Dinosauria, Sauropoda) from southeastern Brazil. Here we provide a detailed revision of all its available specimens, including new elements from the type-locality. One new autapomorphy is added to diagnosis of the taxon: astragalus with a well-developed anteroposterior crest that mediolaterally delimits the tibial articulation. Linear regressions were conducted in an attempt to circumscribe specimens within the type-series, revealing that it is composed of several individuals, with inferred total body lengths varying from 7 to 26 meters. Phylogenetic analyses including *U. ribeiroi* show that the Brazilian taxon corresponds to a non-saltasaurid lithostrotian titanosaur.

Key words: Titanosauriformes, Titanosauria, Phylogeny, South America, Bauru Basin

Introduction

Sauropods can be readily recognized for their typical bauplan, with long necks and tails, columnar members, and gigantic size. First appearing in the Late Jurassic (Wilson, 2006), Titanosauria is the most speciose of all sauropod lineages, with almost 40 species described only from South America (de Jesus Faria *et al.*, 2015). Indeed, titanosaurs are the better known Cretaceous Brazilian dinosaurs (Kellner and Azevedo, 1999; Bittencourt and Langer, 2011), with more than ten described species (e.g., Kellner and Azevedo, 1999; Campos *et al.*, 2005; Kellner *et al.*, 2005; Salgado and Carvalho, 2008; Santucci and Arruda Campos; 2011; Machado *et al.*, 2013; Bandeira *et al.*, 2016). Particularly, three putative species and others to be described come from the Uberaba region (Minas Gerais State; Campos *et al.*, 2005; Kellner *et al.*, 2005; Salgado and Carvalho, 2008). Of these, *Uberabatitan ribeiroi* Salgado and Carvalho, 2008, was the last of those to be described, originally based on three individuals, including cervical, trunk, and caudal vertebrae, scapular and pelvic girdle bones, as well as fore and hind limb elements.

All elements referred to *U. ribeiroi* were unearthed from the same horizon of the “BR-050 B site” (Salgado and Carvalho, 2008; also known as “BR-050 Km 153”, Martinelli and Teixeira, 2015), which belongs to the Serra da Galga Member, Marília Formation, usually dated as Maastrichtian in age (Dias-Brito *et al.*, 2001). As the bones show similar preservation and taphonomic conditions, they were suggested to belong to the same species (Salgado and Carvalho, 2008). Yet, each of the recovered elements received its own collection number (see below) and were split into three individual specimens based only on their gross relative sizes: specimens “A” (considered as the holotype), “B”, and “C”.

The description of *U. ribeiroi* provided by Salgado and Carvalho (2008) was relatively concise and the proposed separation into three specimens rather subjective. Since then, *U. ribeiroi* was included in two phylogenetic analyses (Gallina and Otero, 2015; Bandeira *et al.*, 2016), which did not focus on its relationships. Thus, this contribution aims at providing a detailed anatomical description of all bones referable to *U. ribeiroi* (those already published in addition to new ones) reviewing the inclusivity, relationships, and uniqueness of the taxon based on a comparative approach.

Institutional abbreviations: **CPPLIP**, Centro de Pesquisas Paleontológicas Llewellyn Ivor Price, Universidade Federal do Triângulo Mineiro, Uberaba, Brazil; **MCT**, Museu de Ciências da Terra, Serviço Geológico do Brasil, Rio de Janeiro, Brazil; **MLP**, Museo de La Plata, La Plata, Argentina; **MN**, Museu Nacional, Universidade Federal do Rio de Janeiro, Rio de Janeiro, Brazil; **MPM**, Museu de Paleontologia de Marília, Marília, Brazil; **MPMA**, Museu de Paleontologia Antonio Celso de Arruda Campos, Monte Alto, Brazil.

Systematic paleontology

DINOSAURIA Owen, 1842

SAURISCHIA Seeley, 1888

SAUROPODA Marsh, 1878

TITANOSAURIFORMES Salgado, Coria and Calvo, 1997

TITANOSAURIA Bonaparte and Coria, 1993

UBERABATITAN RIBEIROI Salgado and Carvalho, 2008

Holotype: Following “Article 73.1.5 of the International Code of Zoological Nomenclature (ICZN, 2000)”, CPPLIP-912 (left tibia), CPPLIP-1107 (left fibula), and CPPLIP-1082 (left astragalus) are designated here as composing the redefined holotype of *U. ribeiroi*. They were all parts of the “holotype” as proposed by Salgado & Carvalho (2008), representing the most complete likely articulated set of elements of that series, and are the bearer of two of the proposed autapomorphies of the taxon.

Referred material. Parts of the original holotype: The original “holotype” of *U. ribeiroi* (see Salgado & Carvalho, 2008), also included other elements, which are designated here as referred material: CPPLIP-1058, CPPLIP-1057, CPPLIP-914, CPPLIP-919 (anterior cervical vertebrae); CPPLIP-1091, CPPLIP-1104 (anterior cervical neural arches); CPPLIP-992, CPPLIP-1023 (mid-cervical vertebrae); CPPLIP-993, CPPLIP-915 (posterior cervical centra); CPPLIP-922, CPPLIP-917, CPPLIP-1081, CPPLIP-921, CPPLIP-929, CPPLIP-1105 (cervical ribs); CPPLIP-1077 (anterior dorsal vertebra); CPPLIP-1068 (mid-dorsal neural arch); CPPLIP-923 (dorsal rib); CPPLIP-1099 (sacral centrum); CPPLIP-1079 (anterior caudal vertebra); CPPLIP-1017 (mid-caudal vertebra); CPPLIP-1009, CPPLIP-1010, CPPLIP-1011, CPPLIP-1012 (posterior caudal vertebrae); CPPLIP-1056 (anterior haemal arch); CPPLIP-1006 (posterior haemal arch); CPPLIP-1027 (sternal plate); CPPLIP-1109 (right coracoid); CPPLIP-1030 (left humerus); CPPLIP-1032 (left radius); CPPLIP-911 (right radius); CPPLIP-1080 (right metacarpal); CPPLIP-1029, CPPLIP-1103 (left and right pubes).

Originally referred material: CPPLIP-1075, CPPLIP-1022 (anterior cervical vertebrae); CPPLIP-1085 (anterior/mid-cervical vertebra); CPPLIP-994 (mid-cervical vertebra); CPPLIP-1070 (mid-cervical centrum); CPPLIP-1024, CPPLIP-1108 (posterior cervical vertebrae); CPPLIP-918 (cervical vertebra); CPPLIP-991 (posterior cervical neural arch); CPPLIP-1014 (posterior caudal vertebra); CPPLIP-1078 (fragment of vertebra); CPPLIP-1065 (dorsal rib); CPPLIP-1018 (mid-caudal vertebra); CPPLIP-1019 (mid-caudal vertebra); CPPLIP-1020 (two fused mid-caudal vertebrae); CPPLIP-1008 (posterior caudal centrum); CPPLIP-1005, CPPLIP-1003, CPPLIP-1004 (haemal arches); CPPLIP-1120 (left coracoid); CPPLIP-913 (fragment of right pubis); CPPLIP-1026 (fragment of ischium); CPPLIP-898 (distal end of a left femur); CPPLIP-1106 (left fibula); CPPLIP-1116 (mid-dorsal centrum); CPPLIP-894 (partial right femur).

Newly referred material: six new specimens were recovered from the type-locality of *U. ribeiroi* after the

original specimens were unearthed, they include: CPPLIP-1238 (left femur), CPPLIP-1690 (mid cervical vertebra), CPPLIP-1189 (left femur), CPPLIP-1043 (metatarsal II), CPPLIP-971 (ungual phalanx) and CPPLIP-1691 (proximal chevron).

Observations: The set of materials mentioned above were all found in the type-locality of *U. ribeiroi* and are, based on topotypic principles and agreeing morphology, tentatively associated to that taxon. Yet, the elements show great variation in relative size and, apart from the redefined holotype, have no evidence of articulation. This was corroborated by a linear regression analysis conducted on R environment (Development Core Team, 2013), which allowed the correlation of two continuous variables, the estimated total body lengths of four exceptionally well preserved titanosaurs, *Rapetosaurus krausei* (Rogers and Foster, 2001), *Alamosaurus sanjuanensis* (Tykoski and Fiorillo, 2017), *Dreadnoughtus schrani* (Lacovara *et al.*, 2014), and *Oversaurus paradasorum* (Coria *et al.*, 2013) and the absolute size of 22 of the best preserved bones referred to *U. ribeiroi*, based on the corresponding measurement of the same element in those titanosaurs. The axial elements were measured based on the anteroposterior length of the centra and the appendicular elements on their proximodistal or mediolateral lengths. There is a minimum of five individuals, based on the presence of three left femora of similar medium size (CPPLIP-1238, CPPLIP-1189 and CPPLIP-898), a cervical vertebra of a giant specimen (CPPLIP-1690), and at least one juvenile (see discussion below). Yet, Figure 1 indicates more individuals of different sizes were preserved in the sample.

30

25

20

15

10
5
0

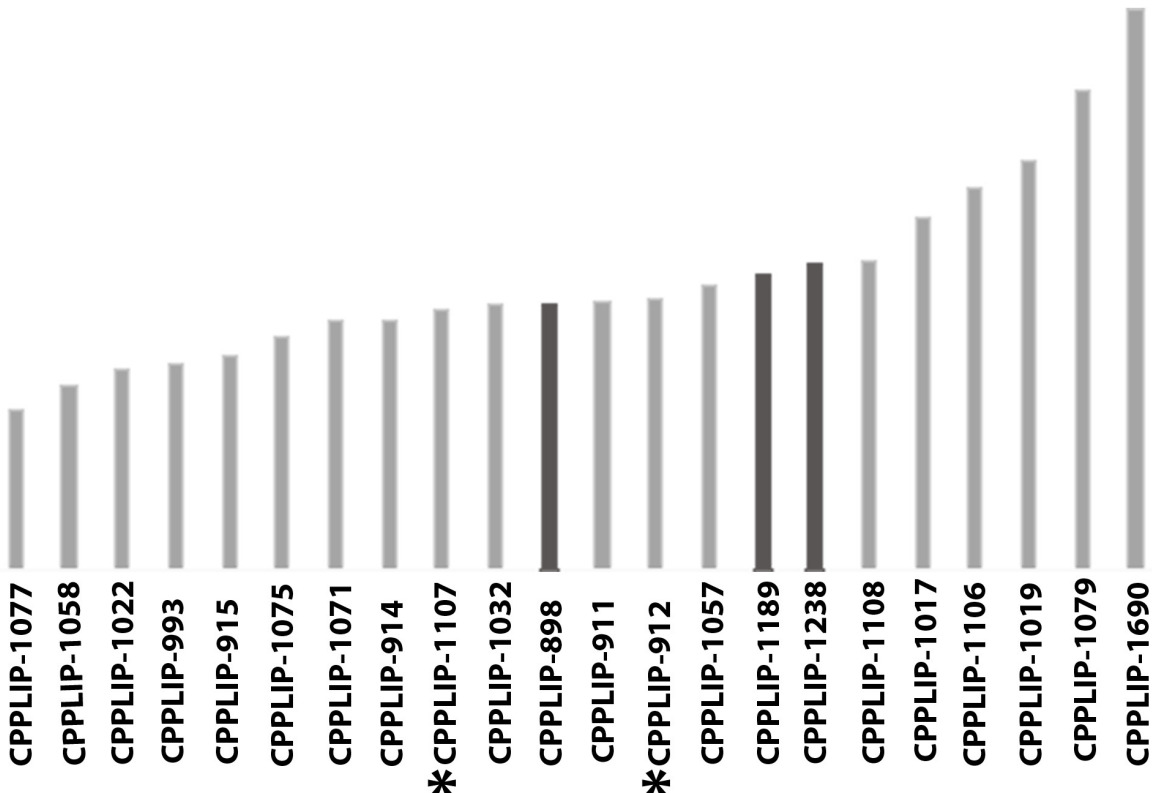


FIGURE 1. Length sizes (m) estimated from several bones referred to *Uberabatitan ribeiroi*. Darksish gray represents the three left femora and the * indicates the redefined holotype.

Revised diagnosis: Salgado and Carvalho (2008) diagnosed *U. ribeiroi* based on a set of autapomorphic features, i.e.: (a) anterior and mid-cervical vertebrae with epipophyseal-prezygapophyseal lamina segmented in two unconnected segments, zygapophyseal and diapophyseal, of which the former extends anterodorsally over the latter; (b) mid-dorsal vertebrae with a robust composite lateral lamina formed mainly by a diapophyseal lamina, probably homologous to the postzygodiapophyseal lamina and, to a lesser extent, by a relic of the spinodiapophyseal lamina; (c) mid (and possibly posterior) dorsal vertebrae with neural accessory laminae parallel

to the prespinal lamina, which are probably the spinoprezygapophyseal laminae; (d) mid-caudal centra with deeply excavated lateral surfaces; (e) pubis with a very stout longitudinal crest on its external (ventral) surface; (f) proximal end of the tibia with a very robust lateral protuberance that articulates with an equally robust medial knob in the fibula. In addition, a new autapomorphy is proposed here: astragalus with a well-developed anteroposterior crest that mediol distally delimits the tibial articulation.

Locality and horizon: All specimens of *U. ribeiroi* were recovered from the same horizon of the “BR-050 B” site (Salgado and Carvalho, 2008), Serra da Galga Member, Marília Formation, considered as Maastrichtian in age (e.g., Dias-Brito *et al.*, 2001), Uberaba, Minas Gerais, Brazil.

Anatomical description. Here we employ the nomenclature proposed by Wilson *et al.* (2011) and Wilson (1999; 2012) to respectively describe the vertebral fossae and laminae of sauropods. For muscular structures and ligaments, we follow the nomenclature proposed by Borsuk-Bialynicka (1977), and Otero and Vizcaíno (2008) for additional hindlimb musculature. For brevity, all monospecific genera will be, from now on, referred only by the generic epithet.

Axial Skeleton

Cervical Vertebrae. Fifteen sauropod cervical vertebrae were recovered from the type-locality of *Uberabatitan*, the exact position of each of them cannot be defined. It is, however, possible to infer the regions to which most of them belong within the neck, i.e. anterior (3 elements), middle (4 elements), or posterior (4 elements), based on traits such as the wider neural canal of more anterior vertebrae and the higher neural spine and more ventrally positioned prezygapophyseal facets of more posterior elements. Four other cervicovertebral elements are too poorly preserved to be properly positioned in the neck.

TABLE 1. Measurements (cm) of the cervical vertebrae of *Uberabatitan ribeiroi*. * = incomplete values; ---- = structure not preserved. **AMCH:** anterior maximum centrum height; **AMCW:** anterior maximum centrum width; **ML:** maximum length; **NSH:** neural spine height; **PMCH:** posterior maximum centrum height; **PMCW:** posterior maximum centrum width.

Specimen	ML	AMCH	AMCW	PMCH	PMCW	NSH
CPPLIP-914	22,70	3,34	4,52	4,90	6,52	----
CPPLIP-915	23,21	----	----	----	----	----
CPPLIP-992	24,40*	----	----	----	----	----
CPPLIP-993	21,53	----	----	----	----	----
CPPLIP-994	23,30*	----	----	9,16	12,15	----
CPPLIP-1016	22,15*	----	----	----	----	----
CPPLIP-1022	23,51	6,30*	13,30*	6,59	11,68	
CPPLIP-1024	22,57*	----	----	8,04	12,50	8,17*
CPPLIP-1057	38,88	4,69*	----	10,43	14,36	10,14
CPPLIP-1058	13,12	4,72*	5,33*	5,17*	4,09*	8,55
CPPLIP-1075	29,37	5,58	6,90	6,12	8,12	----
CPPLIP-1085	39,98	----	----	----	14,21*	11,24*
CPPLIP-1091	32,32	----	----	6,49	10,71	8,33
CPPLIP-1108	40,10	10,77*	16,68*	10,52	16,65	11,53*
CPPLIP-1690	61,58*	13,42	18,21	----	----	17,35

CPPLIP-1058 (anterior cervical vertebra; Fig. 2). The centrum is poorly preserved, with fragmentary condyle and cotyle. Its ventral surface is slightly concave in lateral view, with the anterior margin more dorsally positioned than the posterior. Only small portions of the right parapophysis and left diapophysis are preserved, both positioned ventral to the spinoprezygapophyseal fossa. The inner surface of the pleurocoels is exposed and are shallow. The neural canal has almost half the lateromedial breadth of the centrum. The neural spine is subtriangular in lateral view, with its apex displaced posteriorly and positioned above the cotyle. The spinoprezygapophyseal fossa is wider than those of the other preserved neck vertebrae. It extends along the entire anterior margin of the neural

spine, ending at the anterior edge of the spinopostzygapophyseal fossa, which is deeper than the spinoprezygapophyseal fossa. This last one extends as anteriorly as the anterior opening of the neural canal. Both the pre- and postzygapophyses are structurally similar to those of the best-preserved cervical vertebra (CPPLIP-1057), but their articular facets are wider, with that of the prezygapophyses facing more medially.

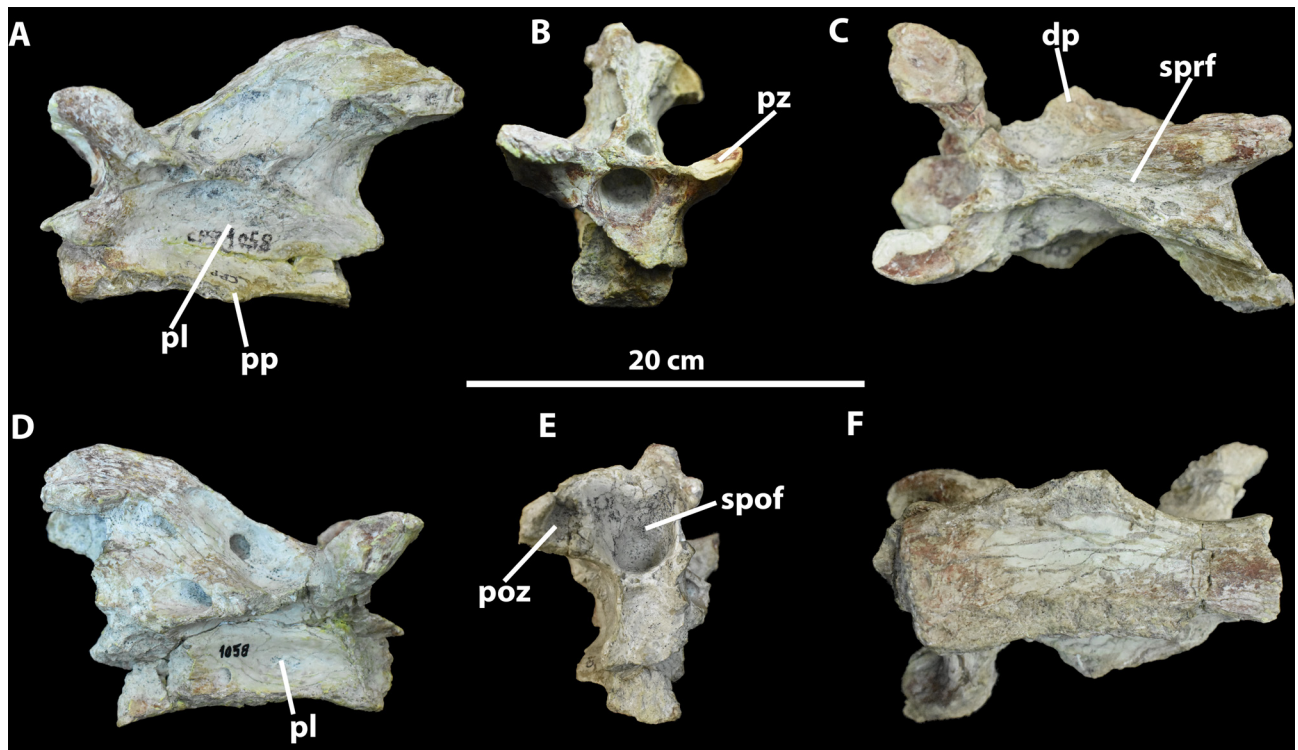


FIGURE 2. Anterior cervical vertebra of *Uberabatitan ribeiroi*. CPPLIP-1058 in **A** left lateral, **B** anterior, **C** dorsal, **D** right lateral, **E** posterior and **F** ventral views. Abbreviations: **dp**: diapophysis; **pl**: pleurocoel; **poz**: postzygapophyses; **pp**: parapophysis; **pz**: prezygapophysis; **spof**: spinopostzygapophyseal fossa and **sprf**: spinoprezygapophyseal fossa.

CPPLIP-914 (partial anterior cervical vertebra; Fig. 3, D1-2). The ventral margin of the centrum is slightly concave in lateral view. The condyle is anteroposteriorly shorter than that of CPPLIP-1057, but the cotyle has similar dimensions. The neural arch is almost entirely lost, only part of the postzygodiapophyseal lamina is visible, along with the spinopostzygapophyseal fossa, which deepens below the postzygodiapophyseal lamina. Only a small portion of the parapophyses is preserved and it extends until the posterior margin of the condyle. The disarticulation of the neural arch suggest that this vertebra may have belonged to a juvenile individual (Martin, 1994; Curry Rogers, 2009).

CPPLIP-1104 (portion of an anterior neural arch; Fig. 3B1-2). Only the left prezygapophysis is preserved. It has a wide, suboval articular facet, which faces strictly dorsally.

CPPLIP-1022 (partial middle cervical vertebra; Fig. 3G). The neural arch is not fused to the centrum. A portion of the right prezygapophysis is preserved. It extends anteriorly beyond the condyle and has an anteroposteriorly large articular facet, with a suboval shape. The right postzygapophysis lacks its articular facet and adjacent laminae. The lateral margin of the left parapophysis is poorly preserved and ventrally borders a deep pleurocoel.

CPPLIP-1075 (partial middle cervical vertebra; Fig. K1-2). This vertebra has the neural arch not fused to the centrum. A portion of the right prezygapophysis is preserved. It extends anteriorly beyond the condyle, but the articular facet is not preserved.

CPPLIP-992 (middle cervical centrum fragment; Fig. 3F). Only the left side of the anterior portion of the vertebra is preserved. On the lateral surface, a small depression represents the pleurocoel. Dorsal to that, a small lamina represents the diapophysis. The parapophysis is partially preserved, and it is larger than those of the best-preserved vertebrae like CPPLIP-1057 and CPPLIP-919. Its long axis is nearly perpendicular to the anteroposterior axis of the centrum. A small portion of the corresponding rib is articulated to the parapophysis.

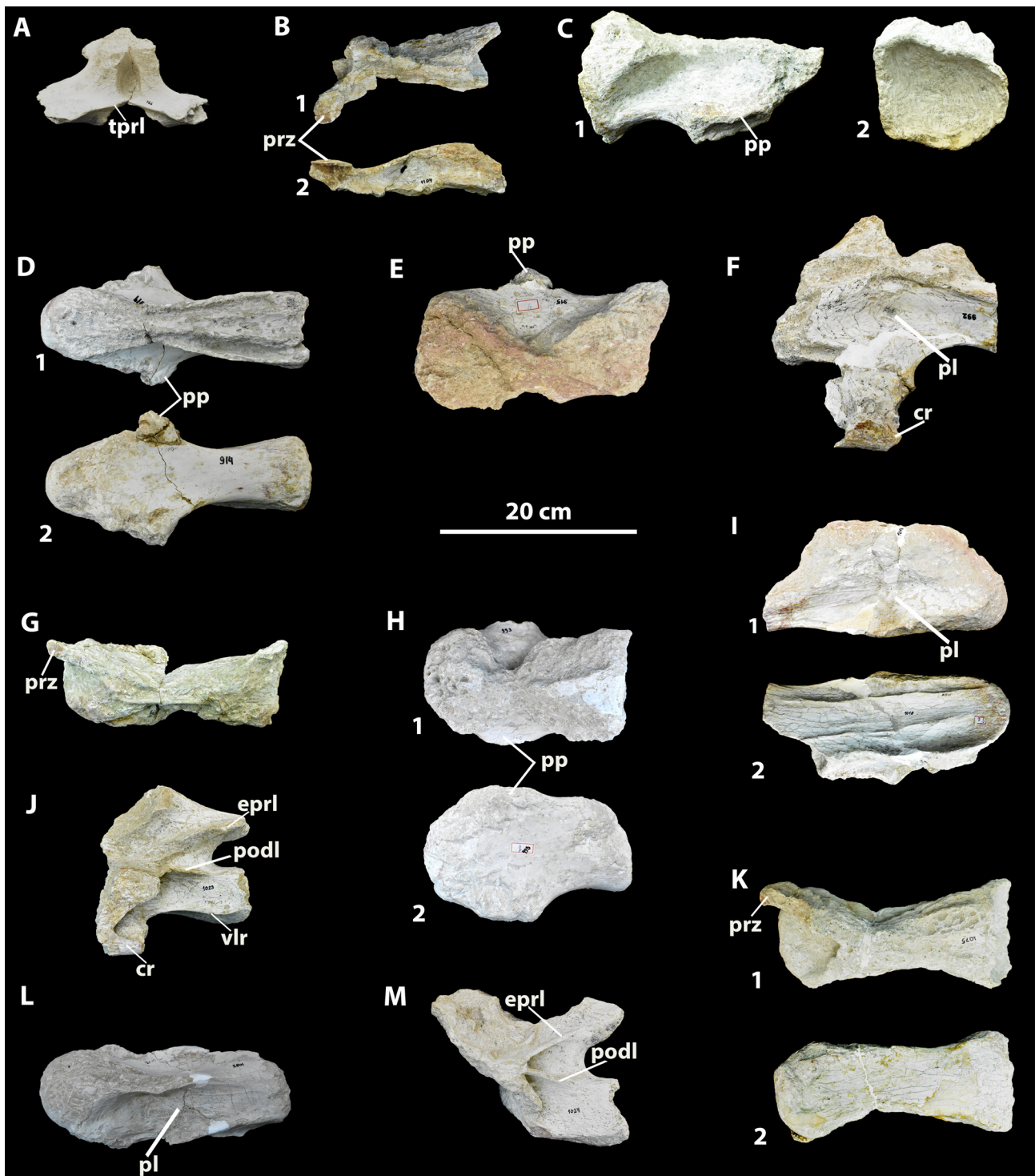


FIGURE 3. Vertebrae of *Uberabatitan ribeiroi*. **A** CPPLIP-991 in anterior view; **B** CPPLIP-1104 in 1, dorsal and 2, left lateral views; **C** CPPLIP-994 in 1, right lateral and 2, posterior views; **D** CPPLIP-914 in 1, dorsal view and 2, ventral views; **E** CPPLIP-915 in dorsal view; **F** CPPLIP-992 in left lateral view; **G** CPPLIP-1022 in dorsal view; **H** CPPLIP-993 in 1, dorsal and 2, ventral views; **I** CPPLIP-1016 in 1, right lateral and 2, ventral views; **J** CPPLIP-1023 in left lateral view; **K** CPPLIP-1075 in 1, dorsal and 2, ventral views; **L** CPPLIP-1085 in left lateral view; **M** CPPLIP-1024 in left lateral view. Abbreviations: **cpol**: centropostzygapophyseal fossa; **cr**: cervical rib; **dp**: diapophysis; **eprl**: epipophyseal-prezygapophyseal lamina; **pl**: pleurocoel; **pocdf**: postzygapophyseal centrodiapophyseal fossa; **podl**: postzygodiapophyseal lamina; **pp**: parapophysis, **prz**: prezygapophysis; **spof**: spinopostzygapophyseal fossa; **spol**: spinopostzygapophyseal lamina; **tprl**: intraprezygapophyseal lamina; **vlr**: ventrolateral ridge.

CPPLIP-1023 (partial middle cervical vertebra; Fig. 3J). Only the left posterior portion of the vertebra is preserved, its overall shape is similar to that of CPPLIP-1057. The main difference is that its ventrolateral ridge is more expanded ventrally than those of the other anterior and middle cervical vertebrae of *Uberabatitan*.

CPPLIP-1057 (middle cervical vertebra; Fig. 4A). This is the best-preserved cervical vertebrae of the sample. The centrum is anteroposteriorly elongated and dorsoventrally short. The short condyle does not extend anteriorly beyond the prezygapophysis. The cotyle is wider than deep, circular in posterior view, and extends as posteriorly as the postzygapophysis. The ventrolateral ridge forms a thin lamina that projects laterally from the ventral margin of the centrum. The ventral surface of the centrum is strongly concave in lateral view, but this feature seems to have been enhanced by taphonomic deformation. The left pleurocoel is shallow, starting from the posterior margin of the condyle, extending below the centropostzygodiapophyseal lamina. The right lateral surface of the vertebra is poorly preserved, showing only a small portion of the postzygapophysis.

On the well-preserved left lateral surface, the prezygapophysis extends anterodorsally, with the articular facet positioned immediately above the condyle. It connects posteromedially with the intraprezygapophyseal lamina, which extends until the anterior margin of the neural canal. The spinoprezygapophyseal lamina separates the spinoprezygapophyseal from the spinodiapophyseal fossae and reaches the neural spine. The latter is triangular in lateral view, displaced posteriorly and expanded mediolaterally. It is anteriorly limited by the spinoprezygapophyseal fossa, which is shallow and extends ventrally until the neural canal. Posteriorly, the neural spine is limited by the spinopostzygapophyseal fossa, which is more excavated at its midlength and also reaches the neural canal. The anterior margin of the spinodiapophyseal fossa becomes deeper in its anterior portion, extending posteriorly until the end of the neural spine and forming the dorsal boundary of the epipophyseal-prezygapophyseal lamina.

The parapophysis is short and slightly bent downwards. It articulates with the cervical rib, forming a perpendicular angle to its main axis. The diapophysis lays posterior to the condyle. It is connected to the centrum via the posterior centrodiapophyseal lamina, situated below the spinodiapophyseal fossa, and to the prezygapophyses by the prezygodiapophyseal lamina. The latter is posteroventrally to anterodorsally directed, reaching above the middle part of the lateral margin of the condyle. The diapophysis is connected to the postzygapophyses via the postzygodiapophyseal lamina, which contacts the epipophyseal portion of the epipophyseal-prezygapophyseal lamina.

The postzygapophyses are located just anterior to the cotyle. Their articular facets are laterally flattened, connected laterally to the neural spine via the zygapophyseal portion of the epipophyseal-prezygapophyseal lamina and to the neural spine via the spinopostzygapophyseal lamina, which extends until the dorsalmost portion of the neural spine. The postzygapophyses are connected by the intrapostzygapophyseal lamina, which has the same lateromedial breadth as the neural canal and separates the spinopostzygapophyseal fossa from the postzygapophyseal centrodiapophyseal fossa, the latter of which is divided in three small fossae.

CPPLIP-1091 (middle cervical vertebra; Fig. 4B). The left surface of the vertebra has all its laminae preserved, which are nearly identical to those of CPPLIP-1057. Exceptions are the more pronounced diapophyseal portion of the epipophyseal-prezygapophyseal lamina and the deeper prezygapophyseal centrodiapophyseal and postzygapophyseal centrodiapophyseal fossae. The articular facets of the prezygapophyses face strictly dorsally, do not extending as anteriorly as in CPPLIP-1057. The condyle is obliterated and the cotyle is taphonomically flattened dorsoventrally, showing well defined edges.

CPPLIP-1690 (middle cervical vertebra; Fig. 5). Only the anterior portion of the vertebra is preserved, its overall shape is similar to those of CPPLIP-1057 and CPPLIP-1091. The main difference is the spinodiapophyseal fossa that it is deeper than that of the other middle cervical vertebrae and also the prezygapophyses, that possess almost half the height of the condyle. Although the left side is not as well preserved as the right, it shows the diapophyseal portion of the epipophyseal-prezygapophyseal, an autapomorphy of *Uberabatitan*.

CPPLIP-1024 (partial posterior cervical vertebra; Fig. 3M). Only the left posterior portion of the vertebra is preserved. The cotyle is deep and has a subcircular shape in posterior view, with well-defined margins. The postzygapophysis bears a large and flat articular facet and is connected with the centrum by a columnar centropostzygapophyseal lamina and with the neural spine by the spinopostzygapophyseal lamina. Laterally, the postzygapophysis is connected with the diapophysis by a thin epipophyseal-prezygapophyseal lamina, which delimits the postzygapophyseal centrodiapophyseal fossa. That fossa excavates medially until close to the neural canal and its limited ventrally by the postzygodiapophyseal lamina.

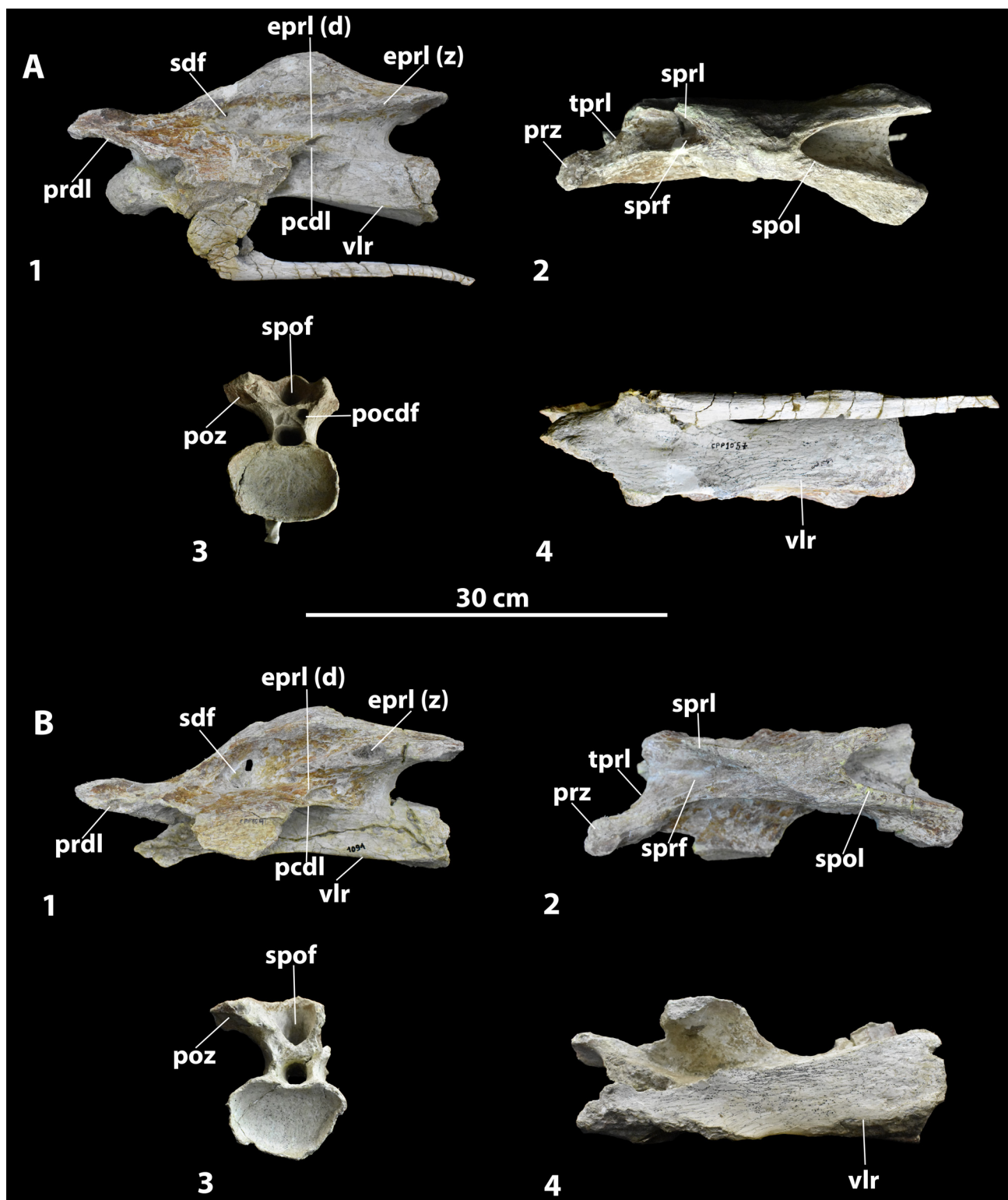


FIGURE 4. Middle cervical vertebrae of *Uberabatian ribeiroi*. **A** CPPLIP-1057 in 1, left lateral, 2, dorsal, 3, posterior and 4, ventral views; **B** CPPLIP-1091 in 1, left lateral, 2, dorsal, 3, posterior and 4, ventral. Abbreviations: **eprl**: epipophyseal-prezygapophyseal lamina (**d**, diapophyseal; **z**, zygapophyseal); **pl**: pleurocoel; **pd़l**: postzygodiapophyseal lamina; **poz**: postzygapophysis; **pocdf**: postzygapophyseal centrodiapophyseal fossa; **prdl**: prezygodiapophyseal lamina; **prz**: prezygapophysis, **sdf**: spinodiapophyseal fossa; **spol**: spinopostzygapophyseal lamina; **sprf**: spinoprezygapophyseal fossa; **tprl**: intrapostzygapophyseal; **vlr**: ventrolateral ridge.

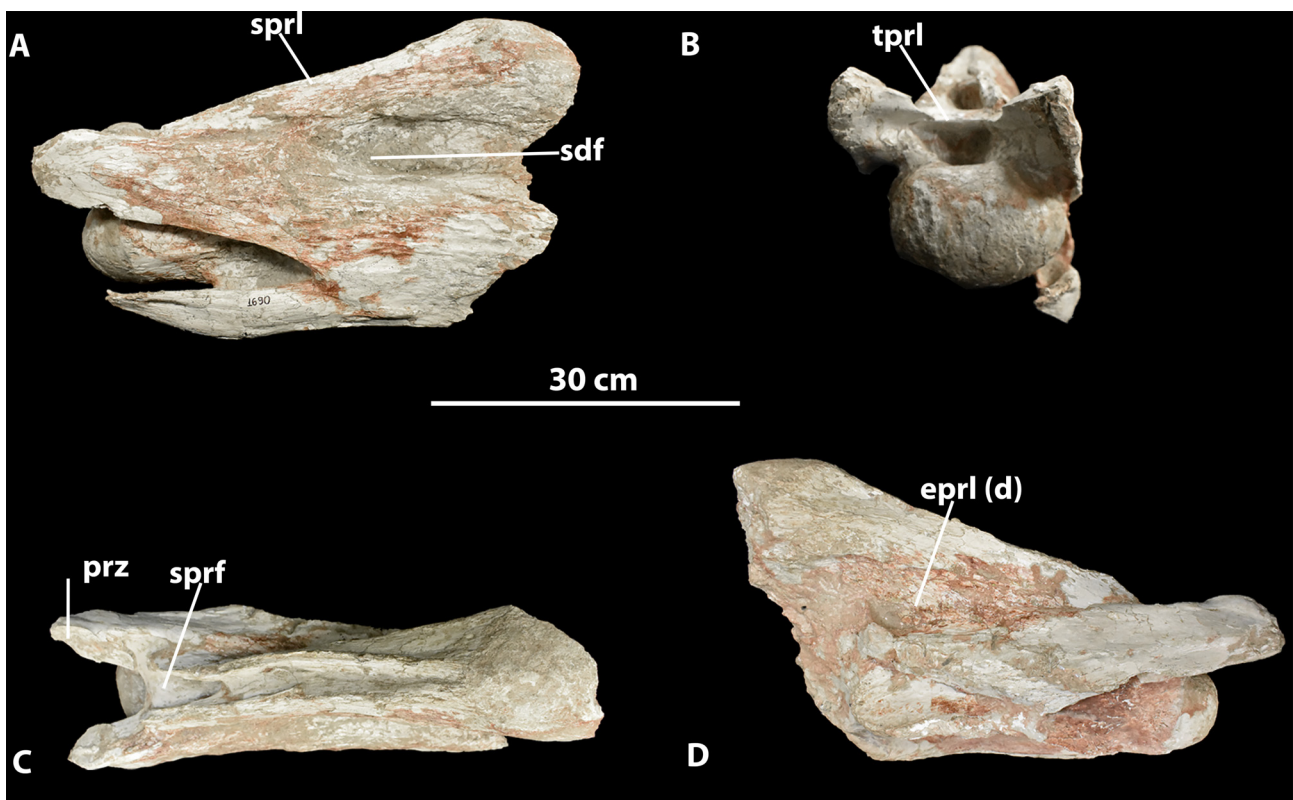


FIGURE 5. Middle cervical vertebra of *Uberabatitan ribeiroi*. CPPLIP-1690 in **A**, left lateral, **B**, anterior, **C**, dorsal and **D**, right lateral views. Abbreviations: **eprl**: Epipophyseal-prezygapophyseal lamina (**d**, diapophyseal); **sdf**: spinodiapophyseal fossa; **sprf**: spinoprezygapophyseal fossa; **tprl**: intraprezygapophyseal lamina.

CPPLIP-991 (posterior cervical neural arch fragment; Fig 3A). Only the anterior part of the neural arch is preserved. The intraprezygapophyseal lamina, is positioned dorsally to a shallow fossa.

CPPLIP-993 (posterior cervical centrum fragment; Fig. 3H1-2). The condyle and cotyle are partially preserved and located at the same dorsoventral level relative to the ventral margin of the centrum, which is slightly concave in lateral view. The proximal portions of both parapophyses are preserved, dorsal to which the pleurocoels are deep and funneled. The inner surface of the posteriormost part of the neural canal is also preserved.

CPPLIP-915 (posterior cervical centrum fragment; Fig. 3E). A small portion of the centrum is preserved, showing a robust condyle that occupies about one third of the total anteroposterior length of the fragment. On the right side, the central portion of a deep pleurocoel is seen. The disarticulation of the neural arch suggest that the centrum may have belonged to a juvenile individual (Martin, 1994; Curry Rogers, 2009).

CPPLIP-1016 (posterior cervical centrum fragment; Fig. 3I1-2). Only a small portion of the left lateral surface of the centrum is preserved, where a large and shallow pleurocoel is seen. Neither the parapophysis nor the diapophysis are preserved.

CPPLIP-1108 (posterior cervical vertebra; Fig. 6). This vertebra is poorly preserved, with fragmented lateral surfaces. The centrum is dorsoventrally short, almost half the depth of the neural arch, with the ventral margin slightly concave in lateral view. The condyle is short and does not surpass the anterior tip of the prezygapophyses. The cotyle is incomplete, missing its ventral portion, but extends posterior to the posterior tip of the postzygapophyses. Only the right prezygapophysis is preserved. It is short and lacks its articular facet. The prezygapophysis is medially connected to the neural arch via the intraprezygapophyseal lamina, which is positioned perpendicular to the neural canal. That zygapophysis also connects to the neural spine via a short epipophyseal-prezygapophyseal lamina and to the centrum via the centroprezygapophyseal lamina. The latter is robust, extending for almost half the dorsoventral depth of the centrum. The neural spine and the central portion of the neural arch are fragmented, with no preserved laminae. Ventral to the neural arch, only the left pleurocoel is preserved. It is shallow and is posteriorly displaced. The right postzygapophysis is poorly preserved and the left one is completely fragmented. Their articular facets are not visible, but are laterally connected to the centrum via

the posterior centrodiapophyseal lamina and medially via the intrapostzygapophyseal lamina, both of which are barely visible due to their poor preservation.

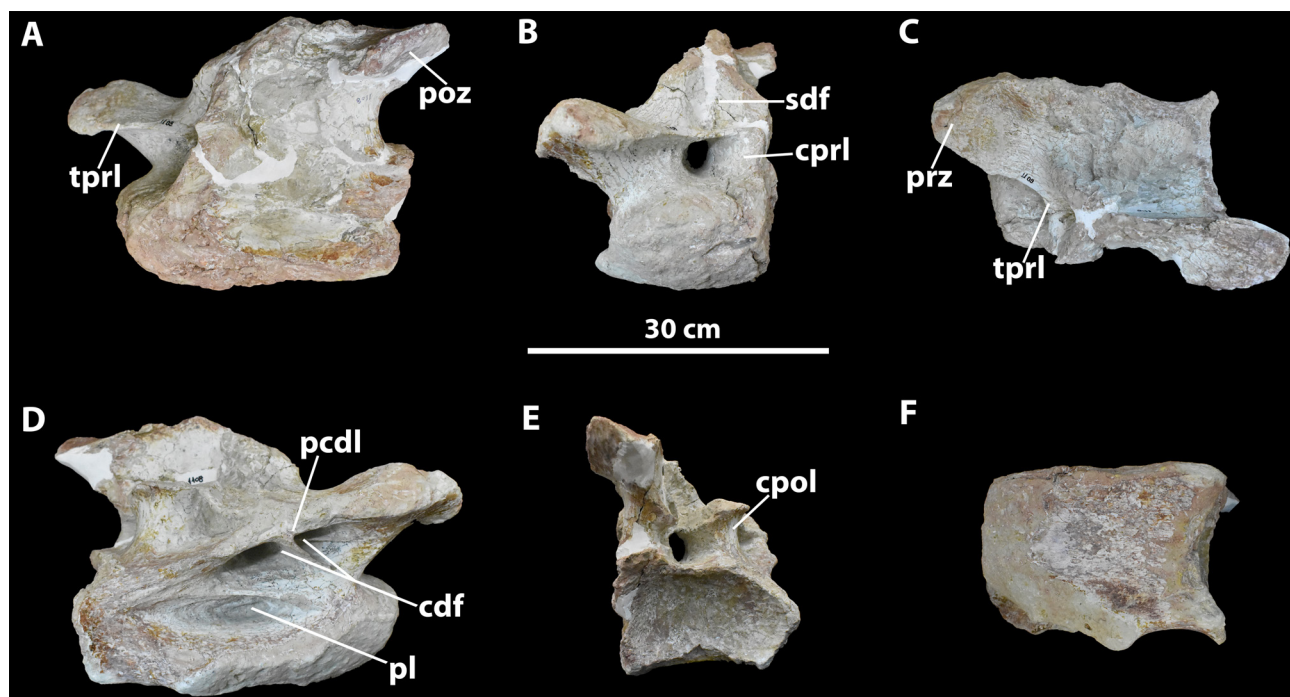


FIGURE 6. Posterior cervical vertebra of *Uberabatitan ribeiroi*. CPPLIP-1108 in **A**, left lateral, **B**, anterior, **C**, dorsal, **D**, right lateral, **E**, posterior and **F**, ventral views. Abbreviations: **cdf**: centrodiapophyseal fossa, **cprl**: centroprezygapophyseal, **cpol**: centropostzygapophyseal fossa, **pcdl**: posterior centrodiapophyseal lamina; **pl**: pleurocoel; **poz**: postzygapophysis, **prz**: prezygapophysis, **sdf**: spinodiapophyseal fossa; **sprf**: spinoprezygapophyseal fossa; **tprl**: intraprezygapophyseal lamina.

CPPLIP-1085 (cervical centrum fragment; Fig. 3L). Only a small portion of the left lateral surface of the centrum is preserved, where a large and shallow pleurocoel is seen. It is limited ventrally by the parapophysis and dorsally by the diapophysis, both poorly preserved.

CPPLIP-994 (cervical centrum fragment; Fig. 3C1-2). Only the cotyle and ventral portion of the centrum are preserved. The former is dorsoventrally shallow, with a rounded outline and poorly defined borders. A small portion of the right parapophysis is preserved, setting the ventral boundary of the pleurocoel.

Trunk Vertebrae. Only two sauropod trunk elements have been recovered from the type-locality of *Uberabatitan*: a nearly complete vertebra from the anterior portion of the series and a more posteriorly positioned fragmentary neural arch.

TABLE 2. Measurements (cm) of the trunk vertebrae of *Uberabatitan ribeiroi*. * = incomplete values; ---- = structure not preserved. **AMCH**: anterior maximum centrum height; **AMCW**: anterior maximum centrum width; **ML**: maximum length; **NSH**: neural spine height; **PMCH**: posterior maximum centrum height; **PMCW**: posterior maximum centrum width.

Specimen	ML	AMCH	AMCW	PMCH	PMCW	NSH
CPPLIP-1068	----	----	----	----	----	23,92*
CPPLIP-1077	9,08	8,61	11,73	8,78	11,08	15,27*

CPPLIP-1077 (anterior trunk vertebra; Fig. 7A). The condyle is robust, expanding anteroposteriorly for one third of the centrum length, and the cotyle has a rounded shape. The lateral and ventral surfaces of the centrum are slightly concave. Only the proximalmost portion of the neural spine is preserved and it is anteriorly limited by the prespinal lamina, which is located on the central portion of the neural arch. The spinoprezygapophyseal lamina extends subparallel to the prespinal lamina and is separated from it by the spinoprezygapophyseal fossa. It is very pronounced and divided in three small laminae when reaching the prezygapophyseal spinodiapophyseal fossa. The

spinodiapophyseal lamina also reaches the spinodiapophyseal prezygapophyseal fossa, on the medial portion of the neural arch.

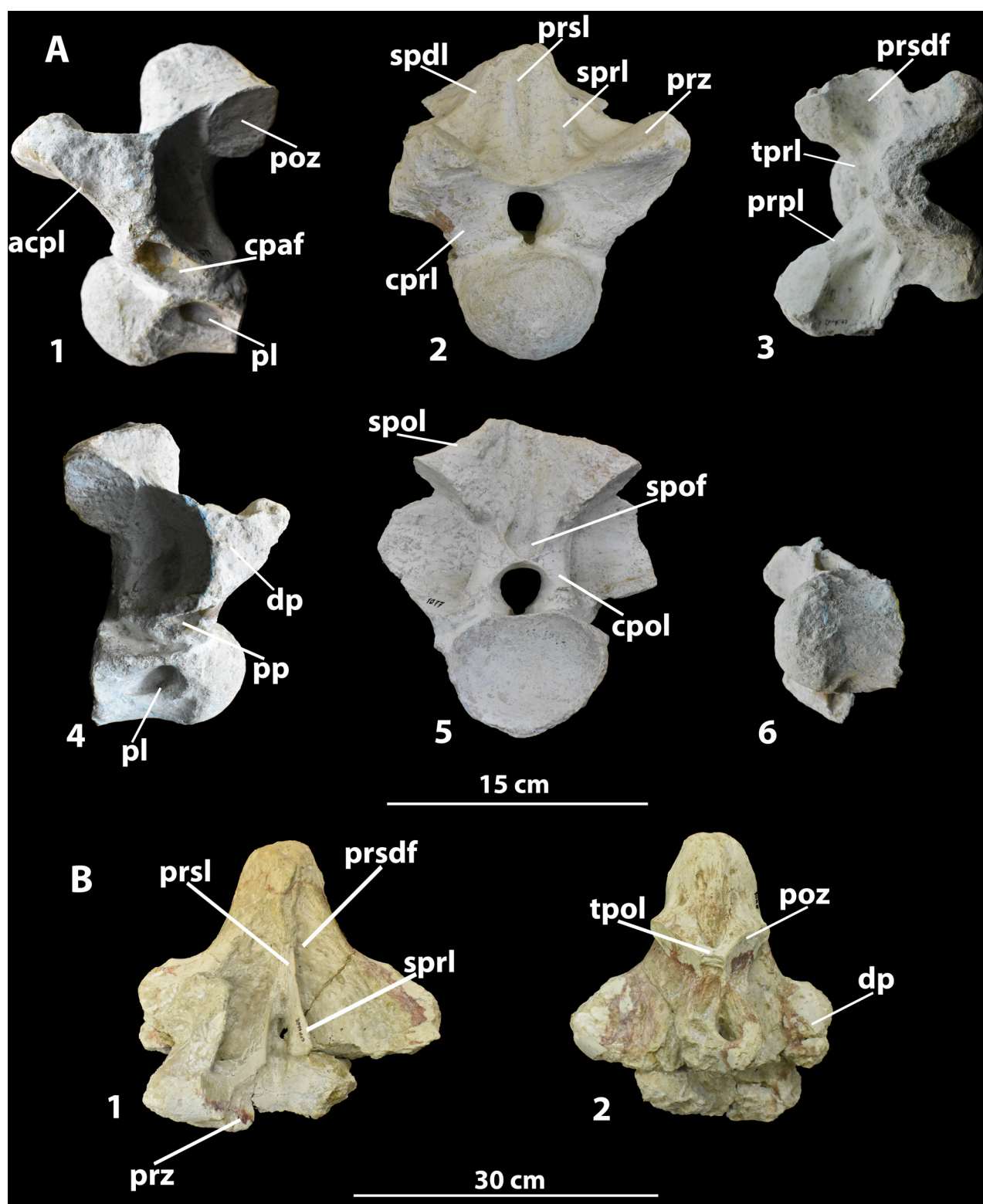


FIGURE 7. Trunk vertebrae of *Uberabatitan ribeiroi*. **A** CPPLIP-1077 in 1, left lateral, 2, anterior, 3, ventral, 4, right lateral, 5, posterior and 6, ventral views; **B** CPPLIP-1068 in 1, anterior and 2, posterior views. Abbreviations: **acpl:** anterior centroparapophyseal lamina; **cpaf:** centroparapophyseal fossa; **cpof:** centropostzygapophyseal fossa; **cprl:** centroprezygapophyseal; **dp:** diapophysis; **pl:** pleurocoel; **pp:** parapophysis; **poz:** postzygapophysis; **prpl:** prezygoparapophyseal lamina; **prsdf:** prezygapophyseal spinodiapophyseal fossa; **prsl:** prespinal lamina; **prz:** prezygapophysis; **spdl:** spinodiapophyseal lamina; **sprl:** spinoprezygapophyseal lamina; **spof:** spinopostzygapophyseal fossa; **spol:** spinopostzygapophyseal lamina; **tpol:** intrapostzygapophyseal; **tpri:** intraprezygapophyseal lamina.

The neural spine is posteriorly limited by the spinopostzygapophyseal lamina, which extends to the postzygapophyses. These are wide, oval in shape, and the articular facets face ventrally. These zygapophyses are connected ventrally with the centropostzygapophyseal lamina, which has almost the same length as the centrum. Between the postzygapophyses, the spinopostzygapophyseal fossa is shallow, and above each of them, the centropostzygapophyseal fossa becomes deeper into the central portion of the neural arch. The pleurocoels are small, anteriorly deep and located on the posterior portion of the centrum, ventral to the anterior centroparapophyseal lamina. They extend below the centropostzygapophyseal lamina. The parapophysis is short and located immediately below the apex of the neural spine. More ventrally, a shallow centroparapophyseal fossa becomes deeper dorsoventrally.

The left prezygapophysis is better preserved than the right. In lateral view, it is perpendicular to the anterior margin of the centrum. Their articular facets are wide, oval, and face dorsally. They are directly in contact to the intraprezygapophyseal laminae. The prezygoparapophyseal lamina extends from the posterior portion of the prezygapophyses to the centroparapophyseal lamina, traversing the lateral surface of the centrum.

CPPLIP-1068 (middle trunk neural arch fragment; Fig. 7B). Only the anteriormost portion of the short prezygapophyses on the right side was preserved. Both portions of the spinoprezygapophyseal lamina converge on the prespinal lamina that extends nearly perpendicular to the prezygapophysis, connecting that structure to the proximal portion of the neural spine. The spinodiapophyseal prezygapophyseal fossa is positioned dorsal to the spinoprezygapophyseal lamina, reaching the diapophysis and becoming deeper close to the prespinal lamina. The postzygapophyses are mediolaterally flattened and separated from one another by a short intrapostzygapophyseal lamina.

Sacral vertebra. A single sacral centrum (CPPLIP-1099; Fig. 8) was recovered from type-locality of *Uberabatitan*. Altogether the sutural surfaces were not preserved, the centrum is relatively well preserved, the disarticulation of the neural arch and sacral ribs may indicate a juvenile specimen (Curry Rogers, 2009). Its ventral surface is slightly concave in lateral view, the lateral surfaces are flat and there is no sign of pneumatization. The condyle is short and has a suboval outline. The cotyle is rounded with poorly defined edges.

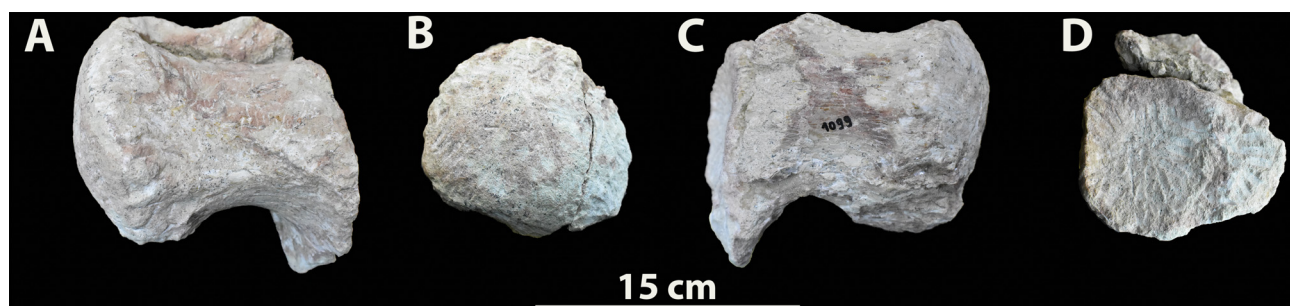


FIGURE 8. Sacral centrum of *Uberabatitan ribeiroi*. CPPLIP-1099 in **A**, left lateral, **B**, anterior, **C**, right lateral and **D**, posterior views.

TABLE 3. Measurements (cm) of the sacral vertebrae of *Uberabatitan ribeiroi*. ---- = structure not preserved. **AMCH**: anterior maximum centrum height; **AMCW**: anterior maximum centrum width; **ML**: maximum length; **NSH**: neural spine height; **PMCH**: posterior maximum centrum height; **PMCW**: posterior maximum centrum width.

Specimen	ML	AMCH	AMCW	PMCH	PMCW	NSH
CPPLIP-1099	16,47	11,76	13,87	11,48	9,04	----

Caudal vertebrae. Eleven sauropod caudal vertebrae were recovered from the type-locality of *Uberabatitan*. Their exact position cannot be defined, but they correspond to three anterior caudal vertebrae, two from the middle of the series, and six more posterior elements.

CPPLIP-1079 (anterior caudal vertebra; Fig. 9). The lateral surfaces of the centrum are slightly concave and the ventral margin is strongly concave in lateral view. As discussed by Salgado and García (2002), the morphology of the caudal vertebrae is highly modified by the caudal musculature, and the excavation in the anterior caudal elements of *Uberabatitan* are related to *M. caudofemoralis longus*, as also seen in *Maxakalisaurus*. The condyle of CPPLIP-1079 is strongly convex, corresponding to almost half of the remaining length of the centrum. The cotyle

is shallow, with a suboval outline, and well-defined edges. A ventrolateral ridge extends anteroposteriorly from the condyle to the cotyle. The neural spine is narrow, flattened and its apex reaches as posteriorly as the condyle. The neural spine is anteriorly connected with each prezygapophysis by a short spinoprezygapophyseal lamina. Both partially preserved transverse processes are laterally projected.

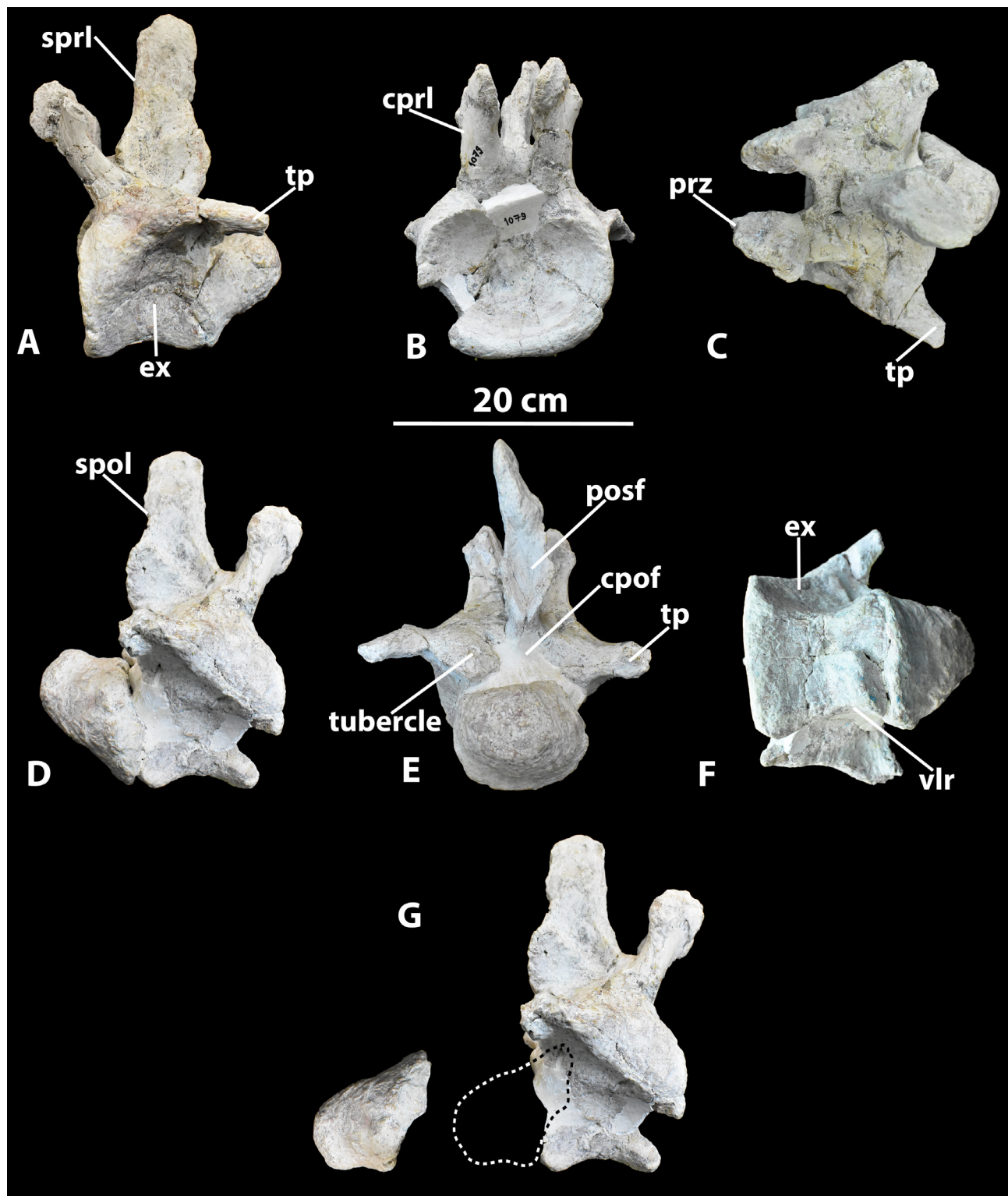


FIGURE 9. Anterior caudal vertebrae of *Uberabatitan ribeiroi*. CPPLIP-1079 as preserved (A-F) and with the condyle digitally restored to its original position (G) in A, left lateral, B, anterior, C, ventral, D,G, right lateral, E, posterior, F, ventral views Abbreviations: **cpof**: centropostzygapophyseal fossa; **cprl**: centroprezygapophyseal lamina; **ex**: excavation; **prz**: prezygapophysis; **spol**: spinopostzygapophyseal lamina; **sprl**: spinoprezygapophyseal lamina; **spof**: spinopostzygapophyseal fossa; **tp**: transverse process; **vlr**: ventrolateral ridge.

TABLE 4. Measurements (cm) of the caudal vertebrae of *Uberabatitan ribeiroi*. ---- = structure not preserved. CPPLIP-1020 are fused and therefore measured together. **AMCH:** anterior maximum centrum height; **AMCW:** anterior maximum centrum width; **ML:** maximum length; **NSH:** neural spine height; **PMCH:** posterior maximum centrum height; **PMCW:** posterior maximum centrum width.

Specimen	ML	AMCH	AMCW	PMCH	PMCW	NSH
CPPLIP-1008	11,73	4,8	7,07	4,78	7,96	2,36
CPPLIP-1009	8,65	6,59	6,07	7,08	4,96	6,52
CPPLIP-1010	12,20	5	6,35	6,12	6,59	2,99
CPPLIP-1011	10,29	3,25	6,52	3,92	5,03	2,83
CPPLIP-1012	6,35	3,26	3,14	3,52	3,52	----
CPPLIP-1014	14,41	6,27	7,54	5,30	8,04	----
CPPLIP-1017	17,13	6,13	6,63	5,63	5,41	7,83
CPPLIP-1019	20,80	10,78	15,89	10,73	14,37	14,64
CPPLIP-1020	30,30	11,19	16,14	11,98	14,86	16,37
CPPLIP-1079	25,10	14,06	16,24	15,74	10,45	21,64

In lateral view, the prezygapophyses are positioned anteriorly to the anterior margin of the centrum, above the cotyle. The articular facets are wide and face medially, with a short intraprezygapophyseal lamina between them. The prezygapophyses are connected to the centrum by an extensive centroprezygapophyseal lamina. In posterior view, the postzygapophyses are short and located anteriorly to the condyle. They have poorly defined articular facets, and a shallow centropostzygapophyseal fossa extends between them along half of the neural spine.

CPPLIP-1017 and CPPLIP-1019 (mid-anterior caudal vertebrae; Fig. 10A–B). These two vertebrae are quite similar, with all structures preserved except for the right prezygapophysis of CPPLIP-1019 and the distal portion of the transverse processes of both elements. Their centra have slightly excavated lateral and ventral surfaces. The latter has four points for the chevron articulation, two below the condyle and two below the cotyle. The condyle extends more posteriorly than the postzygapophyses and has a subquadrangular posterior outline. The cotyle is deep, with well-defined edges. The condyle of CPPLIP-1019 was restored upside down, creating an unnatural angle. The neural spines of both vertebrae are partially preserved, missing their distalmost portions. They are laterally narrow, rectangular in lateral view, and connected to the pre- and postzygapophyses via the spinoprezygapophyseal and spinopostzygapophyseal laminae, respectively. The transverse processes are poorly preserved and located on the anterior portion of the centrum, near the cotyle.

The prezygapophyses are long and dorsoventrally flattened, with the articular facets facing slightly dorsally. These are connected to the centrum via the epipophyseal-prezygapophyseal laminae, which extend until the spinoprezygapophyseal laminae, and are separated by the intraprezygapophyseal lamina. The latter is almost half the width of the centrum. It limits the spinoprezygapophyseal fossae ventrally, which are shallow and together have the same width as the neural canal. The postzygapophyses are short, with wide articular facets facing ventrally and separated by a short intrapostzygapophyseal lamina. The latter has the same width as the neural spine and medially limits the shallow centropostzygapophyseal fossa. The postzygapophyses are connected to the neural arch by the spinopostzygapophyseal lamina, which raises perpendicular to the neural spine in anterior view.

CPPLIP-1020 (fused medial caudal vertebrae; Fig. 11). This set of vertebrae has been extensively discussed by Martinelli *et al.* (2015) focusing on their pathologic condition. The condyle of the more posterior element extends more posteriorly than the postzygapophyses and has a subquadrangular shape in posterior view. The cotyle of the more posterior element is deep and has well-defined edges. The entire lateral surface of the vertebrae is covered with calcified ligaments. The prezygapophyses are long and flattened dorsoventrally, with the articular facets facing slightly dorsally. These are only visible in the more anterior vertebra, as those of the posterior vertebra are fused with the postzygapophyses of the first element. The portions where the prezygapophyses are connected to the centrum are covered with secondary ossification. The neural spine is preserved in both vertebrae, but lacking its apex in the anterior one. The spines are lateromedially narrow and rectangular in lateral view. They connect with the pre- and postzygapophyses via the spinoprezygapophyseal and spinopostzygapophyseal laminae, respectively.

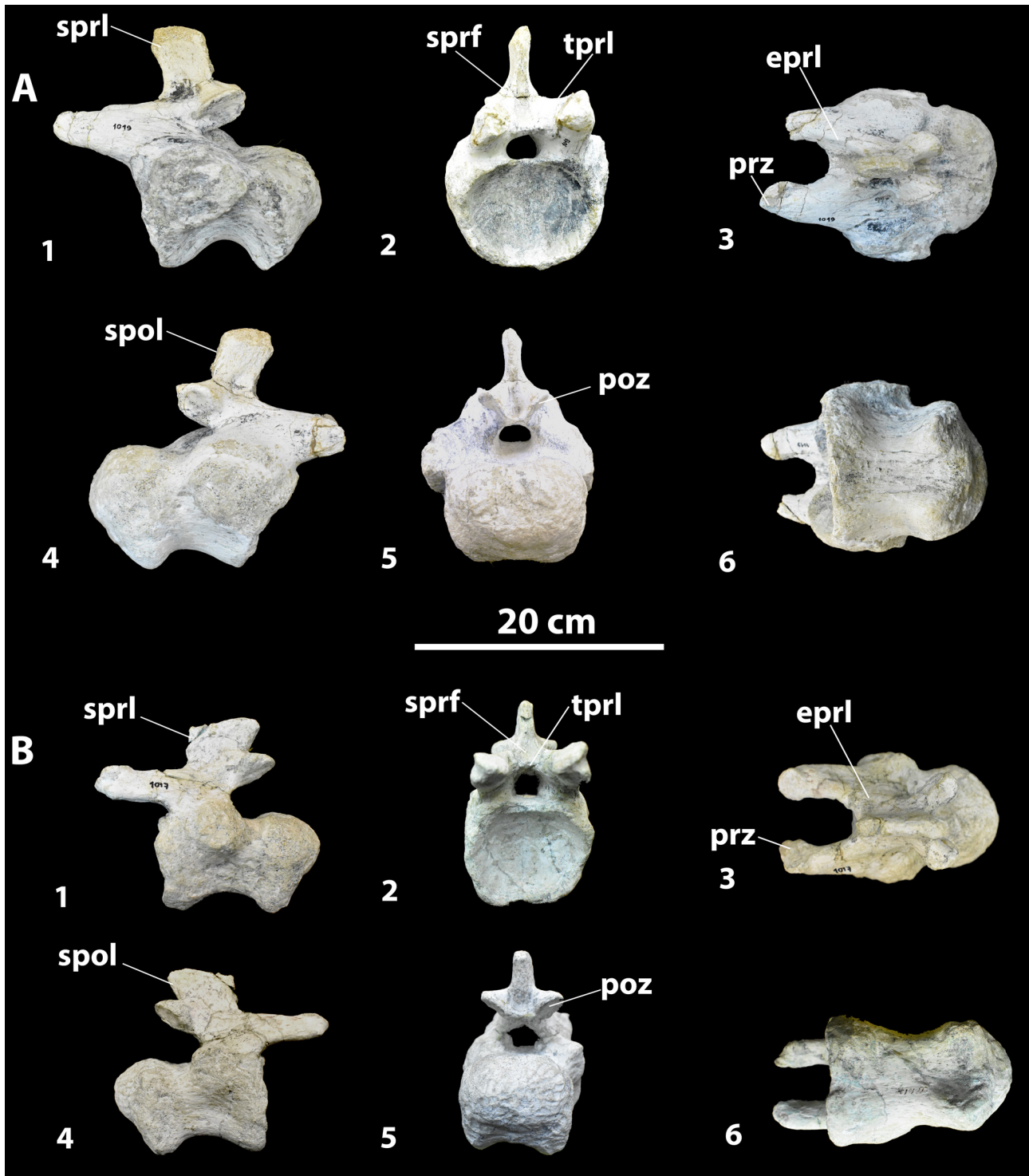


FIGURE 10. Mid-anterior caudal vertebrae of *Uberabatitan ribeiroi*. **A** CPPLIP-1019 in 1, left lateral, 2, anterior, 3, ventral, 4, right lateral, 5, posterior and 6, ventral views; **B** CPPLIP-1017 in 1, left lateral, 2, anterior, 3, ventral, 4, right lateral, 5, posterior and 6, ventral views. Abbreviations: **eprl**: epipophyseal-prezygapophyseal lamina; **poz**: postzygapophysis; **prz**: prezygapophysis; **spol**: spinopostzygapophyseal lamina; **sprf**: spinoprezygapophyseal fossa; **sprl**: spinoprezygapophyseal lamina; **tprl**: intraprezygapophyseal lamina.

CPPLIP-1008, 1009, 1010, 1011, 1012, and 1014 (posterior caudal vertebrae; Fig. 12). The posterior caudal vertebrae are very similar to one another, but have different states of preservation. CPPLIP-1008 lacks the distal portion of the neural spine, the left prezygapophysis, and the distal portion of the right one. CPPLIP-1009 is fully preserved, except for the distal portion of the left prezygapophysis. CPPLIP-1010 lacks the distal portion of the neural spine and the distal portions of both prezygapophyses. CPPLIP-1011 lacks the distal portion of the neural

spine and the distal portion of the left prezygapophysis. CPPLIP-1012 and CPPLIP-1014 have only their centra preserved. In general, the posterior caudal centra are dorsoventrally flattened, with the lateral and ventral surfaces slightly excavated. The condyles and cotyles have subquadrangular anterior/posterior outlines. Only CPPLIP-1008 and CPPLIP-1014 lack protuberances in their ventral surfaces, where the centra articulate with the chevrons. CPPLIP-1010 has a biconcave centrum, whereas the others are procoelic. CPPLIP-1008 lacks well-preserved articulation fates on the prezygapophyses. The posterior caudal neural arches are generally low and positioned at the posterior portion of the centra. The prezygapophyses are short and directly connected with the neural spines, which reach the intrapostzygapophyseal laminae. The postzygapophyses are short, lack well preserved articular facets, and are connected with the centra by the centropostzygapophyseal laminae. The transverse processes of the posterior caudal vertebrae are not well developed.

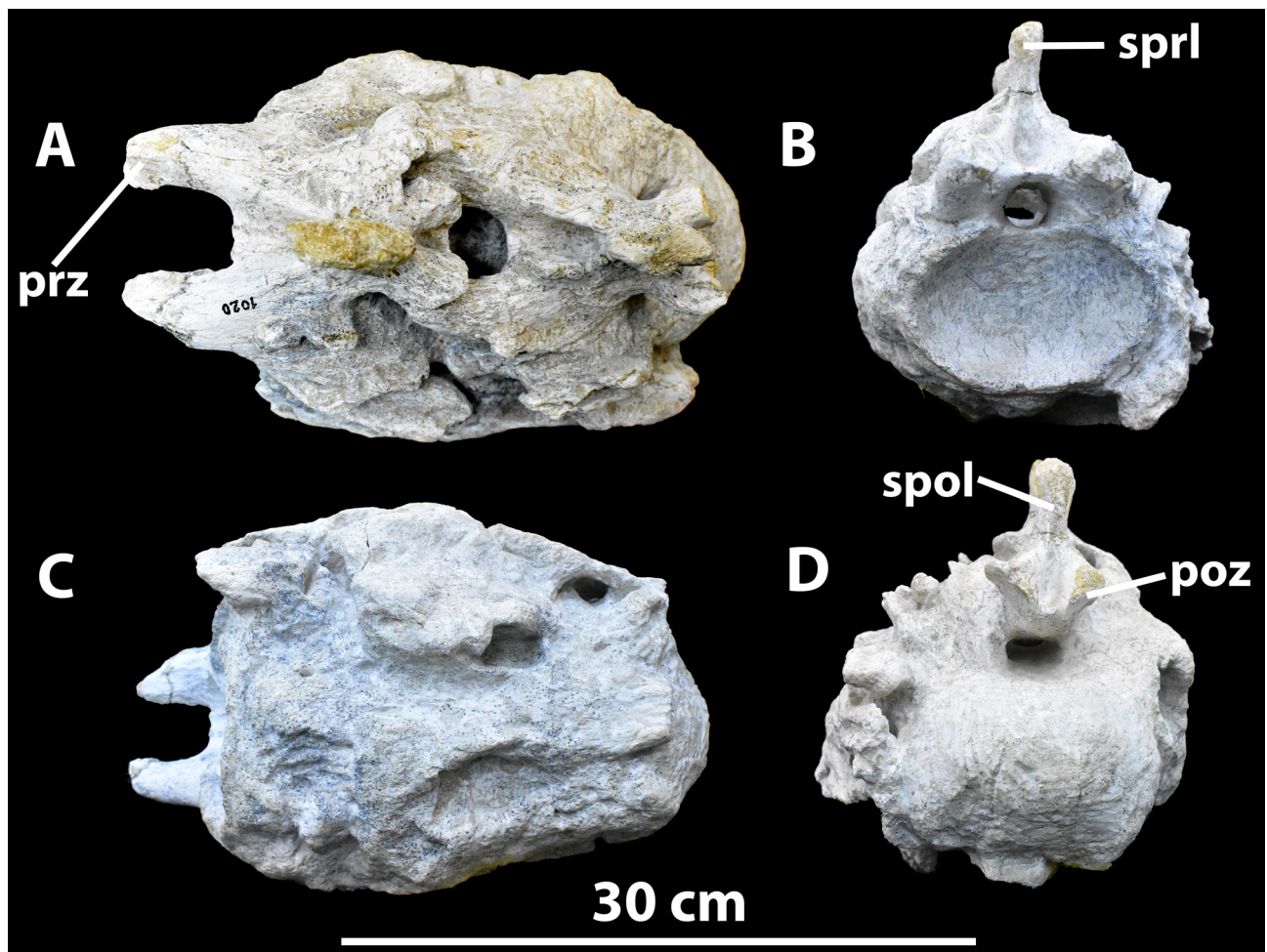


FIGURE 11. Fused mid caudal vertebrae of *Uberabatitan ribeiroi*. CPPLIP-1020 in **A**, dorsal, **B**, posterior, **C**, ventral and **D**, posterior views. Abbreviations: **poz**: postzygapophysis; **prz**: prezygapophysis; **spol**: spinopostzygapophyseal lamina; **sprl**: spinoprezygapophyseal lamina.

Cervical ribs. Isolated and partially preserved cervical ribs include CPPLIP-933, CPPLIP-917, CPPLIP-918, CPPLIP-922, CPPLIP-933, CPPLIP-1052, and CPPLIP-1053 (Figs. 13A-K), whereas cervical vertebrae CPPLIP-918, CPPLIP-919 and CPPLIP-1057 have articulated ribs. All ribs are gracile elements, mainly corresponding to a mediolaterally flattened laminae with a shallow longitudinal excavation on the dorsal surface. The tuberculum of CPPLIP-1057 is a thin and flattened lamina and the capitulum is fragmented.

Trunk ribs. Eight sauropod isolated trunk ribs (Fig. 13L-O) have been recovered in the type-locality of *Uberabatitan*: CPPLIP-923, CPPLIP-927, CPPLIP-929, CPPLIP-923, CPPLIP-1059, CPPLIP-1064, CPPLIP-1087, and CPPLIP-1089. The capitulum and tuberculum are separated and a shallow pneumatic fossa is seen between them. The ribs shafts are flattened and their lateral portion and slightly concave on their medial portion.

Chevrons. Five sauropod chevrons were recovered from the type-locality of *Uberabatitan*. Two from the anterior portion and three from the posterior portion of the tail.

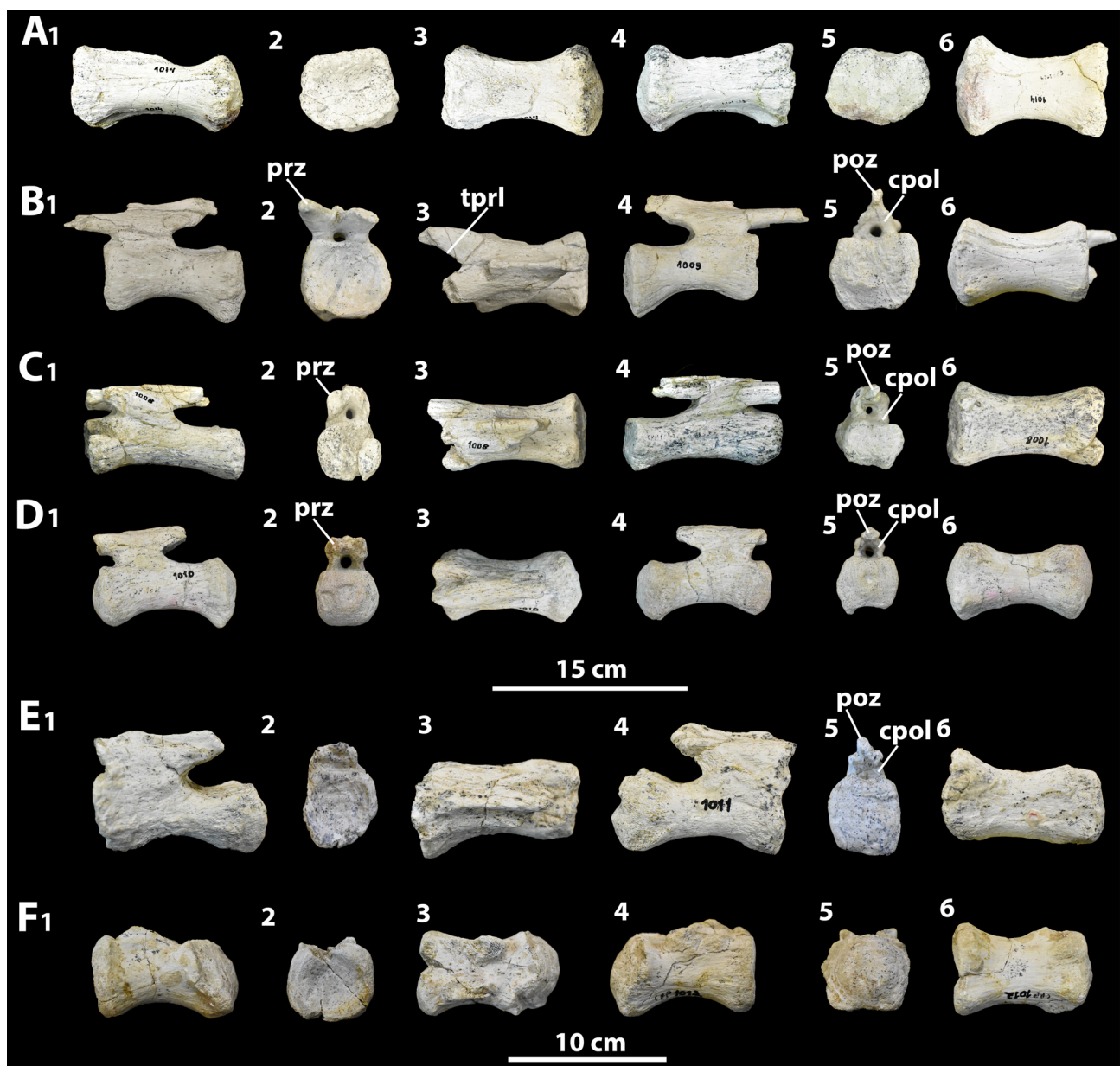


FIGURE 12. Posterior caudal vertebrae of *Uberabatitan ribeiroi*. **A** CPPLIP-1014 in 1, left lateral, 2, anterior, 3, dorsal, 4, right lateral, 5, posterior and 6, ventral views; **B** CPPLIP-1009 in 1, left lateral, 2, anterior, 3, dorsal, 4, right lateral, 5, posterior and 6, ventral views; **C** CPPLIP-1008 in 1, left lateral, 2, anterior, 3, dorsal, 4, right lateral, 5, posterior and 6, ventral views; **D** CPPLIP-1010 in 1, left lateral, 2, anterior, 3, dorsal, 4, right lateral, 5, posterior and 6, ventral views; **E** CPPLIP-1011 in 1, left lateral, 2, anterior, 3, dorsal, 4, right lateral, 5, posterior and 6, ventral views, and **F** CPPLIP-1012 in 1, left lateral, 2, anterior, 3, dorsal, 4, right lateral, 5, posterior and 6, ventral views. Abbreviations: **cpol**: centropostzygapophyseal fossa; **poz**: postzygapophysis; **prz**: prezygapophysis; **tprl**: intraprezygapophyseal lamina.

CPPLIP-1004 and CPPLIP-1056 (anterior chevrons; Figs. 14A-B). The haemal canal is ventrally closed. The articular facets are divided in anterior and posterior portions, which articulate to two adjacent caudal vertebrae. In each chevron, the distal ramus is almost two thirds (65%) the length of the proximal rami. It is mediolaterally flattened, becoming a thin lamina.

CPPLIP-1006, CPPLIP-1005, and CPPLIP-1691 (posterior chevrons; Figs. 14C-E). The articular facets are well marked. CPPLIP-1006 articulated with only one centrum, whereas the other chevrons show articulations with two vertebrae. As in the anterior chevrons, the distal ramus is somewhat larger than the proximal ones. CPPLIP-1006 shows a small protuberance on the left proximal ramus that was recognized as a callus by Martinelli *et al.* (2015).

TABLE 5. Measurements (cm) of the chevrons of *Uberabatitan ribeiroi*.

Specimen	Total height	Proximal rami height	Distal rami height
CPPLIP-1004	38,62	14,82	23,08
CPPLIP-1005	21,90	9,94	11,96
CPPLIP-1006	10,29	5,73	4,56
CPPLIP-1056	32,03	10,77	21,26
CPPLIP-1691	24,35	9,28	15,07

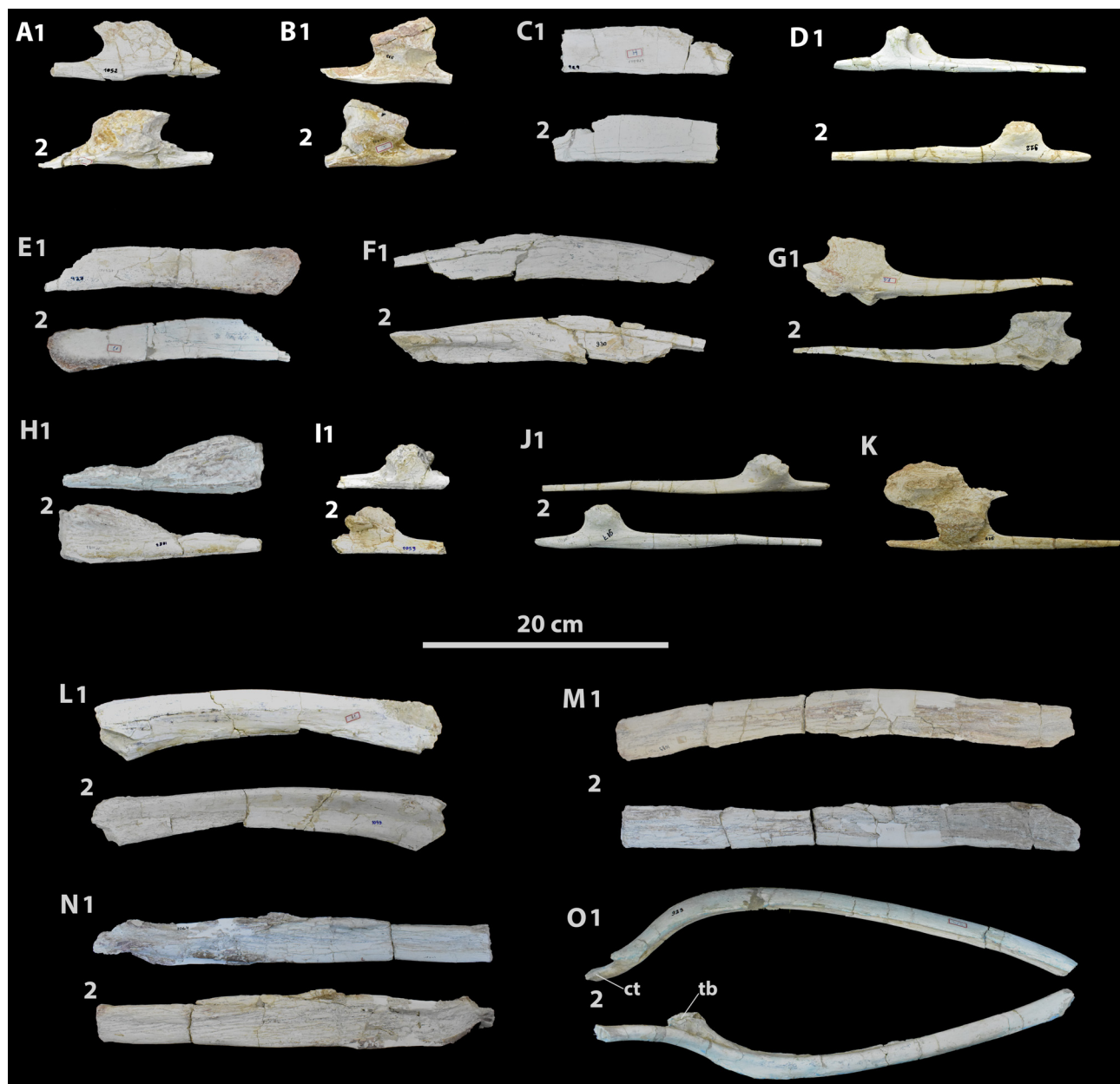


FIGURE 13. Cervical (A-K) and trunk (L-O) ribs of *Uberabatitan ribeiroi*. **A** CPPLIP-1052 in 1, lateral and 2, medial views; **B** CPPLIP-933 in 1, medial and 2, lateral views; **C** CPPLIP-929 in 1, lateral and 2, medial views; **D** CPPLIP-922 in 1, lateral and 2, medial views; **E** CPPLIP-927 in 1, lateral and 2, medial views; **F** CPPLIP-930 in 1, lateral and 2, medial views; **G** CPPLIP-918 in 1, lateral and 2 medial views; **H** CPPLIP-1087 in 1, medial and 2, lateral views; **I** CPPLIP-1053 in 1, medial and 2, lateral views; **J** CPPLIP-917 in 1, medial and 2, lateral views; **K** CPPLIP-919 in left lateral view; **L** CPPLIP-1059 in 1, lateral and 2, medial views; **M** CPPLIP-1064 in 1, lateral and 2, medial views; **N** CPPLIP-1089 in 1, lateral and 2, medial views, and **O** CPPLIP-923 in 1, anterior and 2, posterior views. Abbreviations: **ct**: capitulum; **tb**: tuberculum.



FIGURE 14. Chevrons of *Uberabatitan ribeiroi*. **A** CPPLIP-1004 in 1, anterior, 2, left lateral, 3, distal, 4, posterior and 5, right lateral views; **B** CPPLIP-1056 in 1, anterior, 2, left lateral, 3, distal, 4, posterior and 5, right lateral views; **C** CPPLIP-1691 in 1, anterior, 2, left lateral, 3, distal, 4, posterior and 5, right lateral views; **D** CPPLIP-1005 in 1, anterior, 2, left lateral, 3, distal, 4, posterior and 5, right lateral views, and **E** CPPLIP-1006 in 1, anterior, 2, left lateral, 3, distal, 4, posterior and 5, right lateral views.

Appendicular Skeleton

Titanosaur appendicular elements recovered from the type-locality of *Uberabatitan* include: right and left coracoids, right sternal plate, left humerus, right and left radii, possible metacarpal II, right and left pubes, left ischium, one right and three left femora, left tibia, two left fibulae, left astragalus, possible metatarsal II, and an

ungual phalanx. Except for the specimens assigned to the redefined holotype, all other remains were found disarticulated. Most of the flat bones forming the girdles are incomplete, missing their outer margins.

Pectoral girdle. CPPLIP-1109 and CPPLIP-1120 (right and left coracoids; Fig. 15A–B). Both bones are poorly preserved. The coracoids have a rounded overall shape when seen in dorsal/ventral view. Their dorsal surfaces are slightly concave at the center, and less so near the borders. The glenoid fossa is only partially preserved and it is thickened dorsoventrally. Lateral to that, the margin of the bone extends posteriorly, forming the infraglenoid lip, only preserved on the right coracoid. The coracoid foramen is located on the lateral portion of the bone, ventromedial to the scapular articulation. In ventral view, a small rugosity area posterior to the foramen indicates a possible insertion point for M. costocoracoideus.

TABLE 6. Measurements (cm) of the pectoral girdle elements of *Uberabatitan ribeiroi*.

Specimen	Maximum length	Maximum breadth
CPPLIP-1109 (right coracoid)	33,20	21,35
CPPLIP-1120 (left coracoid)	31,21	14,51
CPPLIP-1027 (right sternal plate)	31,79	9,74

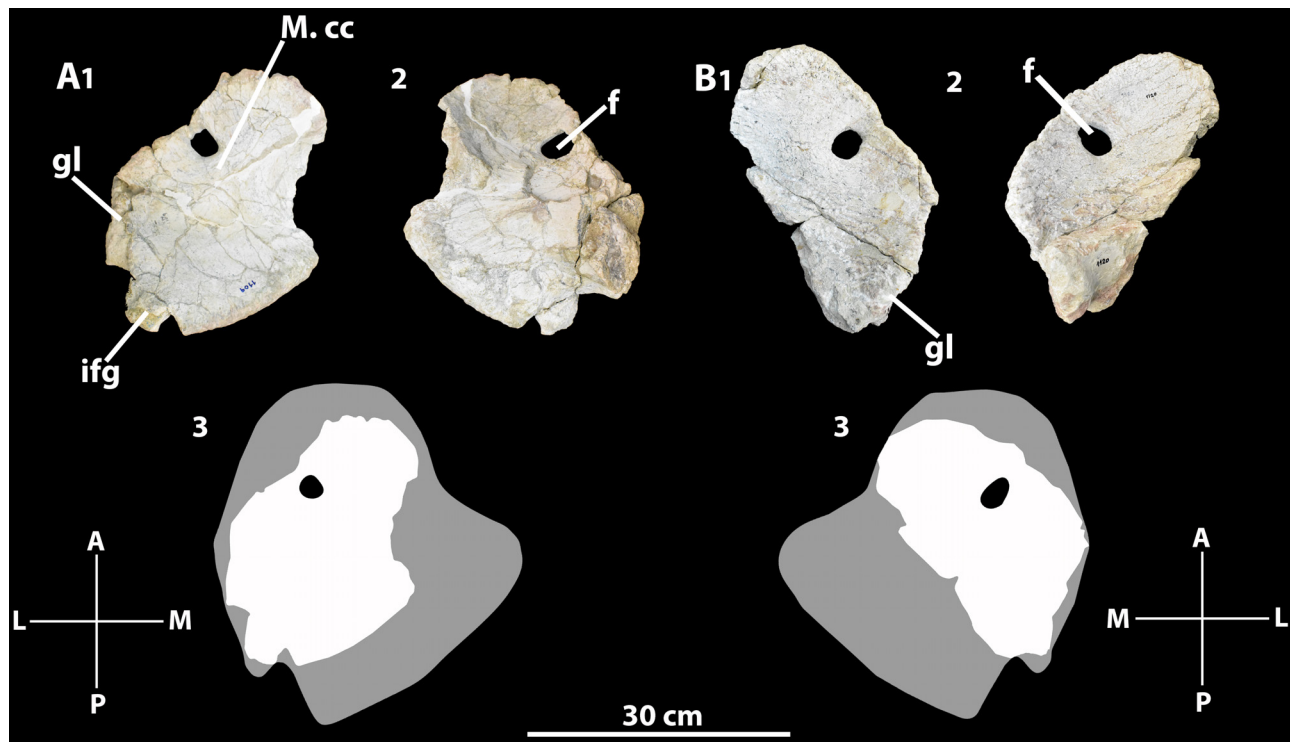


FIGURE 15. Coracoids of *Uberabatitan ribeiroi*. **A**, CPPLIP-1109 in 1, ventral and 2, dorsal views, 3, interpretative draw in ventral view; **B**, CPPLIP-1120 in 1, ventral, and 2, dorsal views; 3, interpretative draw in ventral view. Abbreviations: **gl**: glenoid fossa; **f**: coracoid foramen; **ifg**: infraglenoid lip; **M. cc**: M. costocoracoideus.

CPPLIP-1027 (right sternal plate; Fig 16). The bone is mainly a flat lamina, lateromedially expanded at the anterior margin and lacking the lateral one. The medial border is concave and the posterior end has a ventrally projected protuberance.

Forelimb. CPPLIP- 1030 (proximal portion of a left humerus; Fig. 17). This bone was severely modified by plaster restauration. The deltopectoral crest extends distally from the humeral head along the lateral margin of the bone. Its distal margin was restored in plaster, so that the extension of the crest is unclear. Proximally on the humeral head a small concavity extends mediolaterally, probably representing the insertion point for M. coracobrachialis brevis. The medial border of the head is distally expanded, forming a bulge were where M. pectoralis probably inserted.

TABLE 7. Measurements (cm) of the forelimb elements of *Uberabatitan ribeiroi*. ---- = structure not preserved; * = incomplete measures. **ML:** maximum Length, **MPTB:** maximum proximal transverse breadth, **MPAB:** maximum proximal anteroposterior breadth, **MSB:** maximum shaft breadth, **MDTB:** maximum distal transverse breadth and **MDAB:** maximum distal anteroposterior breadth.

Specimen	ML	MPTB	MPAB	MSB	MDTB	MDAB
CPPLIP-911 (right radius)	47,25	12,78	6,78	6,16	13,56	8,63
CPPLIP-1030 (left humerus)	48,69*	36,17	16,08	----	----	----
CPPLIP-1032 (left radius)	50,75	14,79	10,07	4,93	14,58	9,48
CPPLIP-1080 (left Metacarpal II)	30,17	6,90	5,11	3,94	7,38	4,55

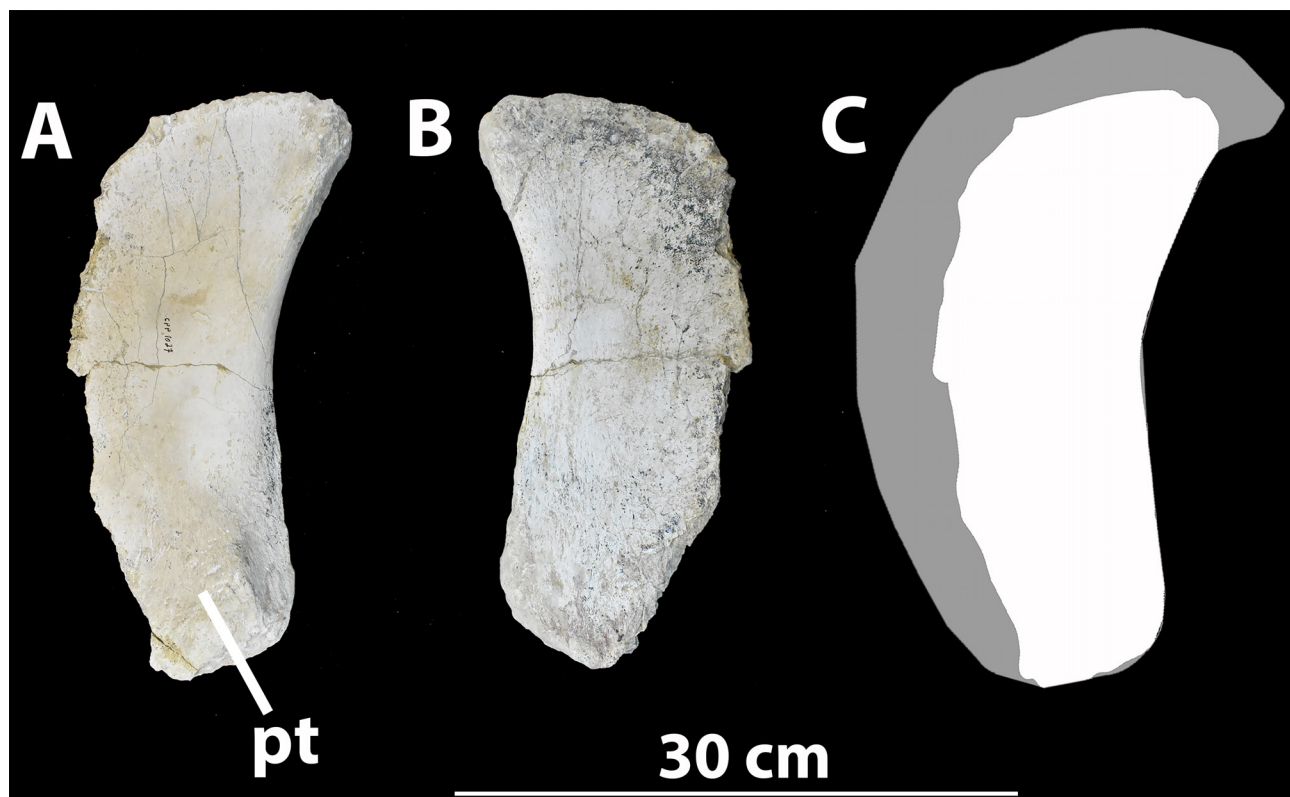


FIGURE 16. Sternal plate of *Uberabatitan ribeiroi*. CPPLIP-1027 in **A**, ventral and **B**, dorsal views. **C**, interpretative draw in ventral view. Abbreviations: **pt**: protuberance.

CPPLIP-911 and CPPLIP-1032 (right and left radii; Fig. 18). Both radii are very similar in shape and preserved structures. The bone arches outwards in anterior/posterior views and has a rounded proximal margin. The proximal and the distal ends are similarly mediolaterally expanded. The proximal articular surface is flat, whereas the distal is concave and beveled in medial/lateral views, with a rugose surface. In lateral view, where the ulna radius articulates, there is a crest extending longitudinally along almost the entire medial surface of the bone. This crest is formed by the interosseous ridge for the attachment of an interosseous membrane between the two bones (Curry Rogers, 2009). The distal ulnar articular facet is rounded and expands laterally. That of the right radius is thinner mediolaterally than that of left bone. The distal end expands lateromedially and is anteroposteriorly flattened. In anterior view, the bone surface is flat at mid-shaft, becoming slight concave distally, proximal to the distal end, where *M. flexor carpi radialis* inserted.

CPPLIP-1080 (left metacarpal II; Fig. 19). The proximal articular surface of the bone is flat and quadrangular in proximal view. The distal articular surface is rugose, has a semicircular distal outline, and lacks a distal articular facet for the phalanx. In anterior view, the proximal articulation is slightly concave. On the medial surface, a small protuberance is seen more proximally, where the bone articulated with metacarpal I. More distally, the shaft becomes concave laterally and bears an anteriorly projected crest that extends proximodistally from the distal end

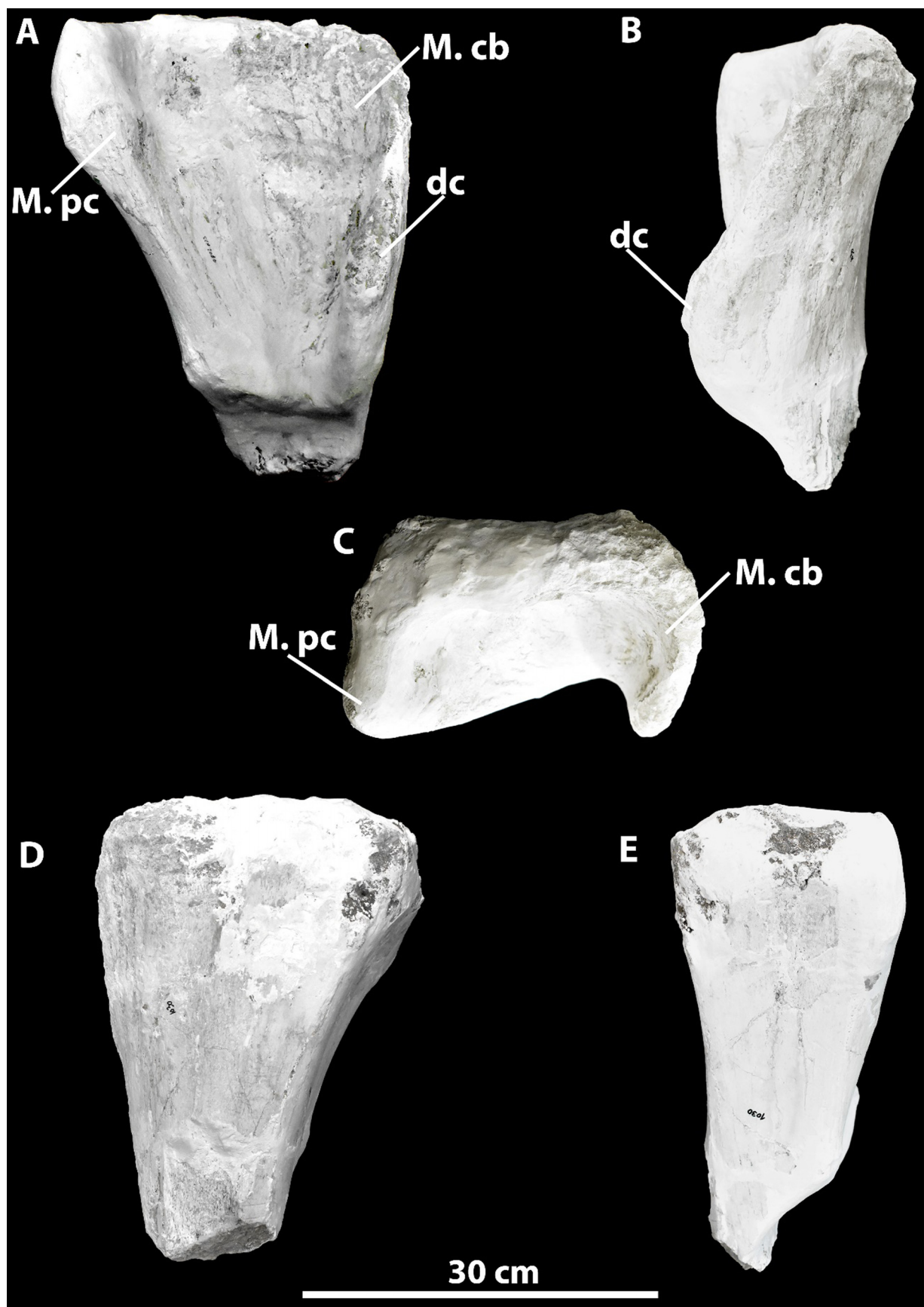


FIGURE 17. Humerus of *Uberabatitan ribeiroi*. CPPLIP-1030 left humerus in **A**, anterior; **B**, medial; **C**, proximal; **D**, posterior and **E**, lateral views. Abbreviations: **dc**: deltopectoral crest; **M. cb**: insertion for the *M. coracobrachialis brevis*; **M. pc**: insertion for the *M. pectoralis*.

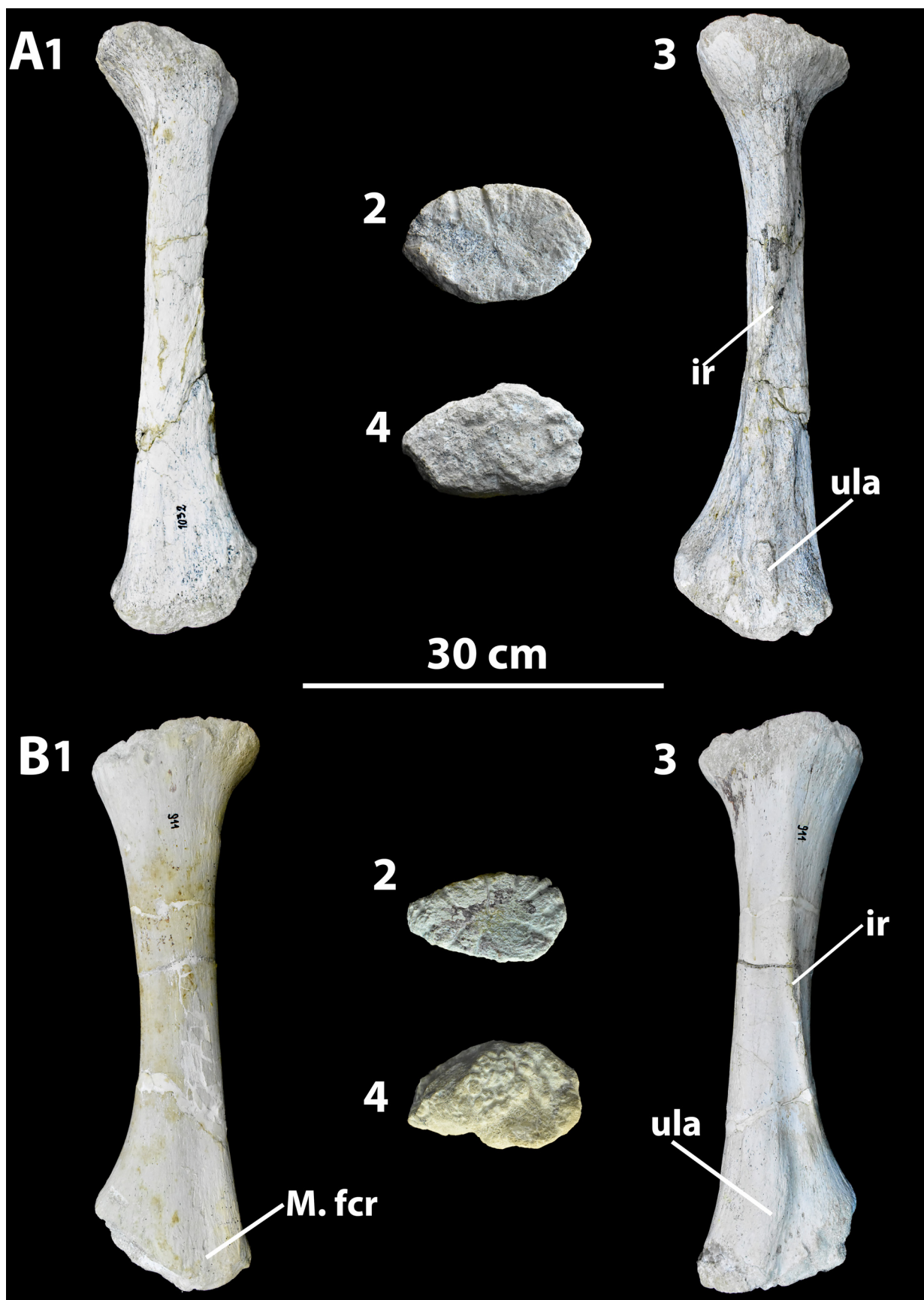


FIGURE 18. Radii of *Uberabatitan ribeiroi*. A, CPPLIP-1032 right radius in 1, anterior, 2, proximal and 4, distal views; B, CPPLIP-911 left radius in 1, anterior, 2, proximal, 3, posterior and 4, distal views. Abbreviations: **ir**: interosseous ridge; **M. fcr**: insertion for the *M. flexor carpi radialis*; **ula**: ulnar articular facet.

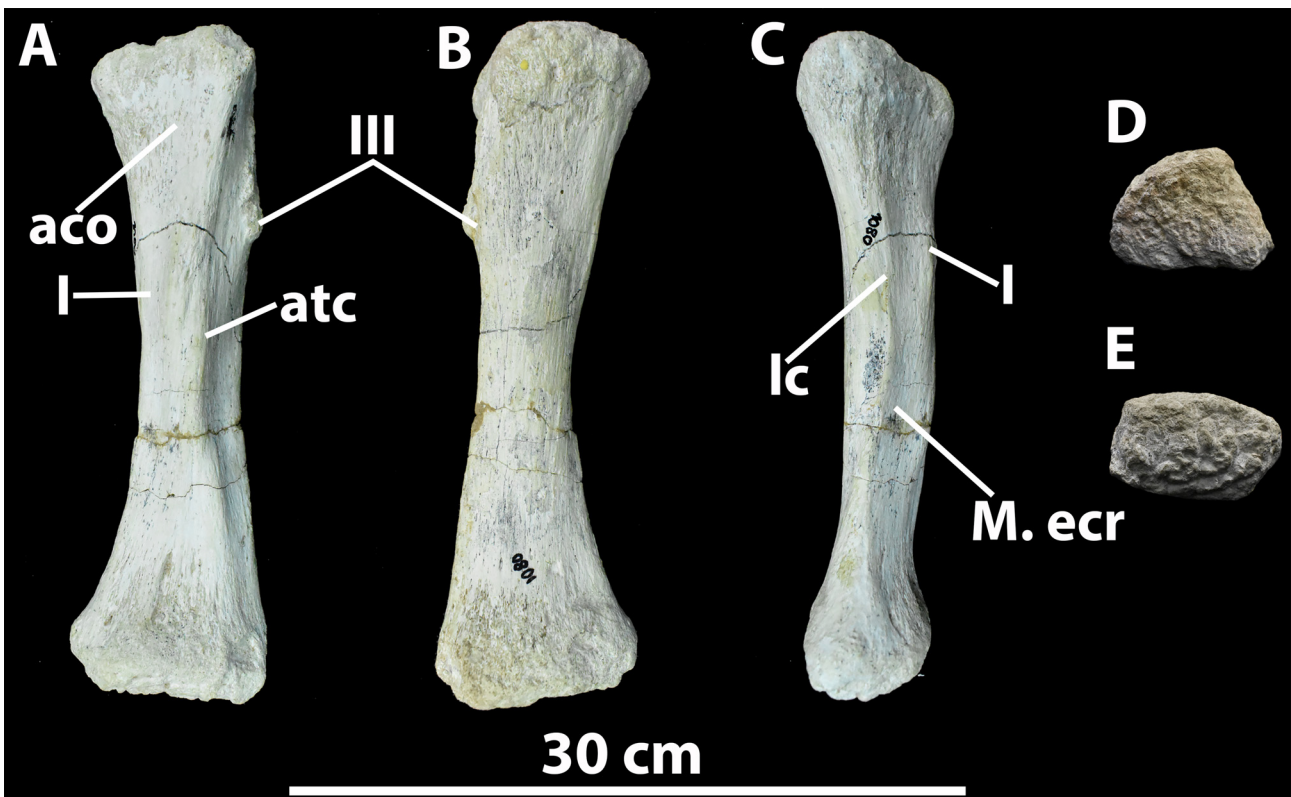


FIGURE 19. Metacarpal II of *Uberabatitan ribeiroi*. CPPLIP-1080 in A, anterior, B, posterior, C, medial, D, proximal and E, distal views. Abbreviations: I: articulation with metacarpal I; III: articulation with metacarpal III; aco: anterior concavity, atc: anterior crest; lc: longitudinal crest, M. ecr: insertion for the M. extensor carpi radialis.

towards the midshaft axis. Another small lateral crest extends longitudinally along the proximal third of the bone, where it articulated with metacarpal III. On the medial surface, a small crest extends longitudinally along the proximal portion of the bone. Distal to that, the surface becomes slightly concave, where M. extensor carpi radialis inserted.

Pelvic Girdle. CPPLIP-1029 and CPPLIP-1103 (left and right pubes; Fig. 20). CPPLIP-1029 preserved parts of its proximal portion, whereas CPPLIP-1103 has only the distal portion preserved. The proximal portion of the bone is lateromedially expanded. The obturator foramen is wider dorsoventrally than anteroposteriorly. The ventral surface of the pubis is concave and the lateral one bears a crest that extends proximodistally. This crest is more robust in CPPLIP-1029 than in the CPPLIP-1103, and possibly was the attachment site for the dorsal portion of M. puboischiofemoralis externus. Neither the ischial and iliac peduncles, nor the ambiens process and the symphyseal portions are preserved.

TABLE 8. Measurements (cm) of the pelvic girdle elements of *Uberabatitan ribeiroi*.

Specimen	Maximum length	Maximum breadth
CPPLIP-1029 (left pubis)	59,28	15,18
CPPLIP-1103 (right pubis)	54,23	18,13
CPPLIP-1026 (right ischium)	27,11	13,74

CPPLIP-1026 (proximal portion of a right ischium; Fig. 21). Only part of the iliac process is preserved, corresponding to a mainly laminar flat element. Its medial surface bears a rugose region that probably represents one of the insertions of M. flexor tibialis. The lateral surface of the bone is flat.

Hindlimb. CPPLIP-1238 (complete left femur; Fig. 22A), CPPLIP-1189 (distal portion of a left femur; Fig. 22B), CPPLIP-894 (proximal portion of a right femur; Fig. 22C), and CPPLIP-898 (distal portion of a left femur; Fig. 22D). The femora are robust, similar in most details, and here described together with the differences cited

whenever necessary. The femoral head of *Uberabatitan* is strongly convex in lateral/medial views, slightly projected proximally, and beveled in anterior/posterior views. It projects dorsal to the level of the great trochanter. The anterior surface of the shaft is flat with a crest extending dorsoventrally along the midshaft, ending on the tibial condyle. This corresponds to the linea intermuscularis cranialis (Otero, 2010), which bounds the insertion site for M. femorotibialis internus medially and that for M. femorotibialis externus laterally. Lateral to that, the fourth trochanter is visible in anterior/medial views. It is composed by a small lamina positioned about 40% the length of the femur from its proximal margin, projecting more posteriorly than the femoral head. Although poorly developed, it offered the attachment site for both Mm. caudofemoralis brevis and longus. The posterior surface of the shaft is limited laterally by the lateral bulge, which extends dorsoventrally below the femora head. Medially to the bulge, there is a small proximodistally elongated depression, which represents the insertion site for M. ischiotrochantericus. Starting posterior to this depression, the trochanteric shelf extends distally, parallel to the lateral projection of the great trochanter, until the level of the fourth trochanter. At mid-shaft, the femur has a subcircular cross-section, slightly compressed anteroposteriorly. In the distal portion of the bone, the tibial and fibular condyles are pronounced and have similar proportions, with the latter mediolaterally longer than the former. The postolateral fossa forms a shallow groove on the posterior portion of the fibular condyle, creating a slightly developed medial ridge. Both condyles project posteriorly to the femoral head and also lateromedially beyond the shaft margins in anterior/posterior views.

TABLE 9. Measurements (cm) of the hindlimb elements of *Uberabatitan ribeiroi*. ---- = structure not preserved; * = incomplete measures. **ML:** maximum length, **MPTB:** maximum proximal transverse breadth, **MPAB:** maximum proximal anteroposterior breadth, **MSB:** maximum shaft breadth, **MDTB:** maximum distal transverse breadth, and **MDAB:** maximum distal anteroposterior breadth.

Specimen	ML	MPTB	MPAB	MSB	MDTB	MDAB
CPPLIP-894 (right femur)	45,89*	----	----	----	----	----
CPPLIP-898 (left femur)	38,12*	----	----	----	36,74	21,27
CPPLIP-912 (left tibia)	59,67	19,90	15,03	8,87	16,22	11,02
CPPLIP-1034 (left metatarsal II)	13,52	7,26	4,84	3,82	2,97	5,78
CPPLIP-1106 (left tibia)	65,54*	----	----	6,43	13,16*	9,18*
CPPLIP-1107 (left tibia)	55,13	17,44	9,49	5,24	8,57	11,02
CPPLIP-1189 (left femur)	54,05*	----	----	----	17,27	9,85
CPPLIP-1238 (left femur)	66,29	23,16	11,28	10,98	21,68	14,25

TABLE 10. Additional measurements (cm) to the pedal elements of *Uberabatitan ribeiroi*.

Specimen	Maximum length	Maximum height	Maximum breadth
CPPLIP-971 (ungual phalanx)	13,93	12,43	13,98
CPPLIP-1082 (left astragalus)	9,84	9,14	6,33

CPPLIP-912 (redefined holotype; left tibia; Fig. 23A, D). The medial surface of the tibial shaft is flat and the bone expands both at its proximal and distal portions. In lateral/medial view, the proximal portion has a squared shape, where a shallow posterolateral fossa is visible. The lateral surface has a lateral protuberance at its proximal portion that articulated with the proximal portion of the fibula. The proximal articulation is composed mainly by a single bulge, with a shallow depression where it articulates with the femur. The cnemial crest projects laterally and becomes wider anteroposteriorly in its middle portion. It is a very robust structure that supported the triceps tendon. Posterior to the cnemial crest, there is no sign of a ‘second cnemial crest’ (Bonaparte *et al.*, 2000). Laterally, between the cnemial crest and the tibial protuberance, there is a small depression extending proximodistally, where M. extensor digitorum communis inserted. Distal to this depression, the shaft slightly arches medially until it widens due to the presence of a crest that expands proximally from the anterior margin of the distal portion, right proximal to the lateral condyle. The medial surface of the distal portion of the tibia bears a triangular shaped tuberosity that articulated to the astragalus. The distal end of the tibia is poorly preserved and neither the lateral or medial malleolus are preserved.

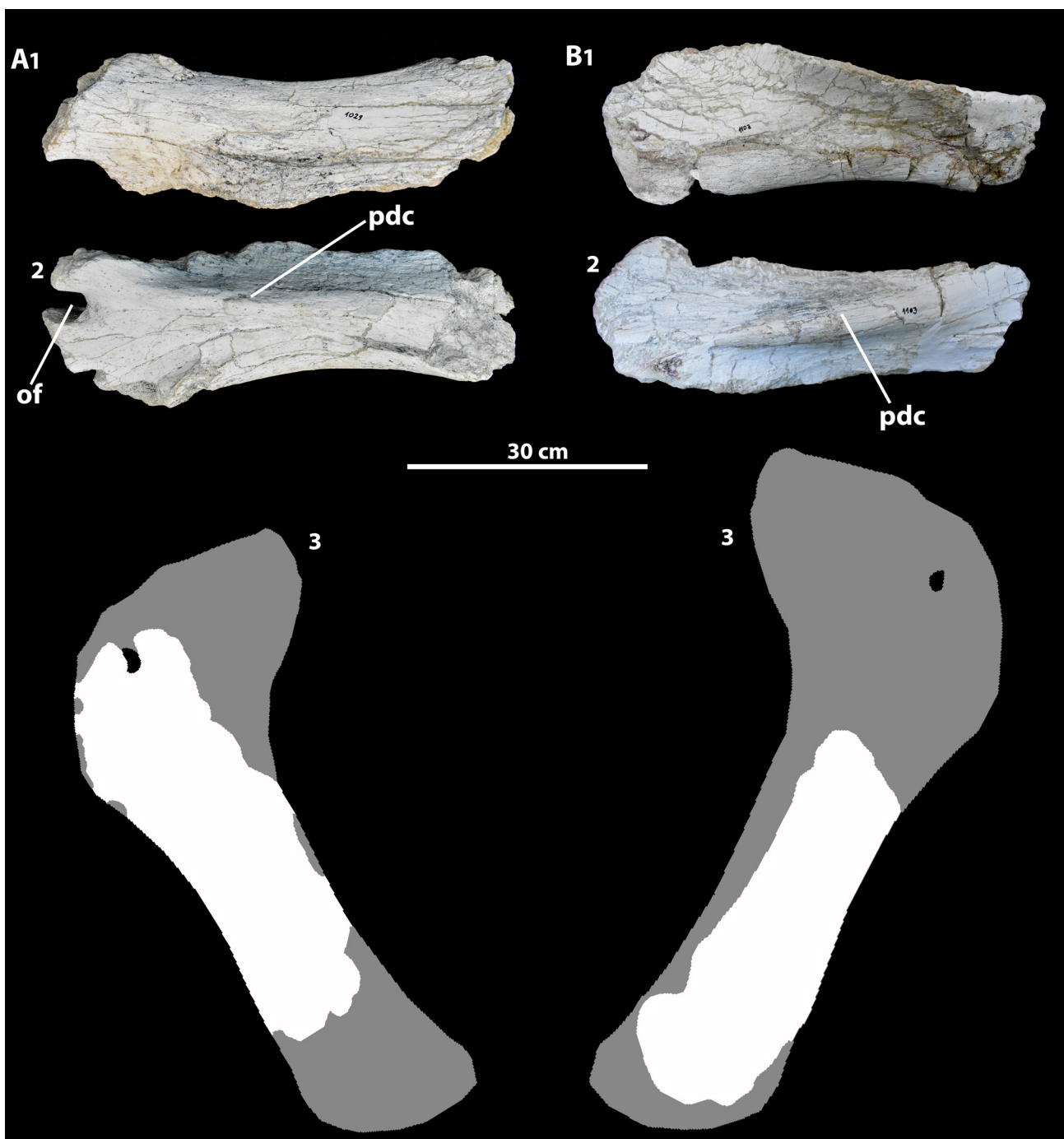


FIGURE 20. Pubis of *Uberabatitan ribeiroi*. **A**, CPPLIP-1029 on 1, dorsal; 2, ventral views and 3, interpretative drawn on ventral view; and **B**, CPPLIP-1103 on 1, dorsal; 2, ventral views and 3, interpretative drawn on ventral view. Abbreviations: **pdc**: proximodistal crest, **of**: obturator foramen.

CPPLIP-1107 (redefined holotype; left fibula; Fig. 23B, D) and CPPLIP-1106 (left fibula, Fig. 23C). The fibulae of *Uberabatitan* are gracile elements compared to the tibia. Both fibulae are here described together with the differences cited whenever necessary. CPPLIP-1107 is completely preserved and CPPLIP-1106 lacks only its most proximal portion. The proximal portion of the bone is very expanded anteroposteriorly and has a rugose proximal articular surface, where the fovea ligamentosa was inserted medially and the joint capsule laterally. In lateral view, the lateral trochanter forms a large protuberance, projecting more laterally from mid-shaft than the margins of both the proximal and distal articulations. The lateral trochanter is flanked posteroproximally by the attachment site for *M. iliofibularis*, from which it is separated by an oblique ridge, and distally by a rugose area for the origin of *M. flexor digitorum longus* (Curry Rogers, 2009). The medial surface of the fibula is flat and the

fibular knob has a triangular shape in medial view. The bone has a triangular shape in distal view, and the corresponding articular surface is slightly concave.

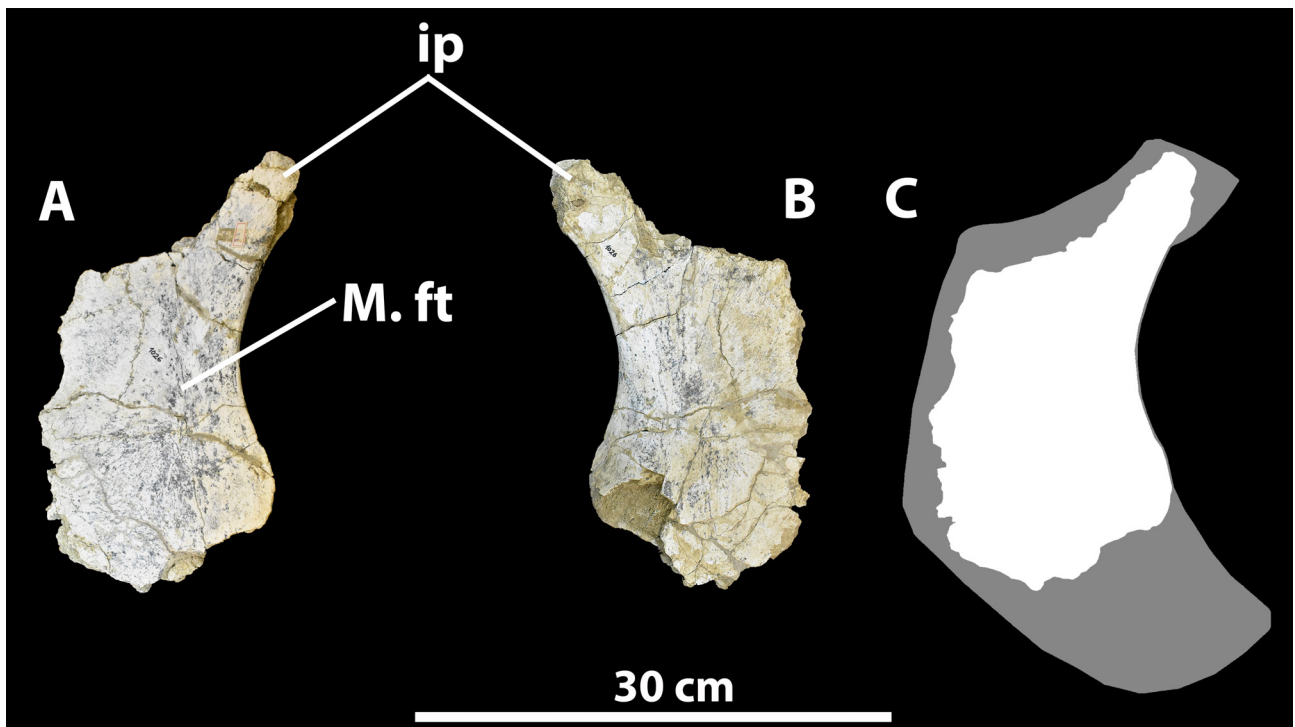


FIGURE 21. Ischium of *Uberabatitan ribeiroi*. CPPLIP-1026 on **A**, medial, **B**, lateral views and **C**, interpretative drawn on medial view. Abbreviations: **M. ft**: insertion for the *M. flexor tibialis*; **ip**: ischial peduncle.

CPPLIP-1082 (redefined holotype; left astragalus; Fig. 24A). The astragalus is subtriangular in proximal view, with nearly straight anterior, posteromedial, and posterolateral margins. The tibial and fibular articulations are separated by a robust anteroposteriorly elongated ridge. The tibial articulation is placed on a small concavity delimited mediadistally by a well-developed crest that extends anteroposteriorly. The fibular articulation is a well-marked concavity, twice the size of the tibial one. The distal surface of the bone is strongly rugose and gently curves anteriorly, being somewhat continuous to that surface.

CPPLIP-1034 (left metatarsal II; Fig. 24B). The identity of the metatarsal can be inferred based on the shape of its proximal articular surface compared to that of complete pes such as that of the “La Invernada” titanosaur (González Riga *et al.*, 2008), where that articulation is typically subrectangular in proximal view. The proximal portion of the bone is lateromedially expanded. In dorsal view, on the proximal portion of the shaft, there is a small tubercle that delimits medially the articular region with the first metatarsal. The bone is rounded in distal view and has a concave articular surface.

CPPLIP-971 (ungual phalanx; Fig. 24C). This element is poorly preserved, lacking its distal tip. The phalanx is mediolaterally compressed and its plantar surface is strongly concave.

PHYLOGENETIC ANALYSES

In order to evaluate the phylogenetic position and relationships of *Uberabatitan* we performed a phylogenetic analysis based on modifications of the taxon/character matrices of Martínez *et al.* (2016) and González Riga *et al.* (2018). *Uberabatitan* was scored from both the redefined holotype and all referred material. The first matrix was analyzed in TNT 1.5 (Goloboff *et al.*, 2016) with tree bisection and reconnection (TBR) as the branch swapping algorithm, hold established as 20, 5,000 replicates, and random seed as “0”. The latter matrix was analyzed with the *Stabilize Consensus* option in the New Technology search on TNT. Sectorial searches were performed, employing drift and tree fusing, with the consensus stabilized five times, and the resulting trees used as starting trees for Tradicional search using TBR.

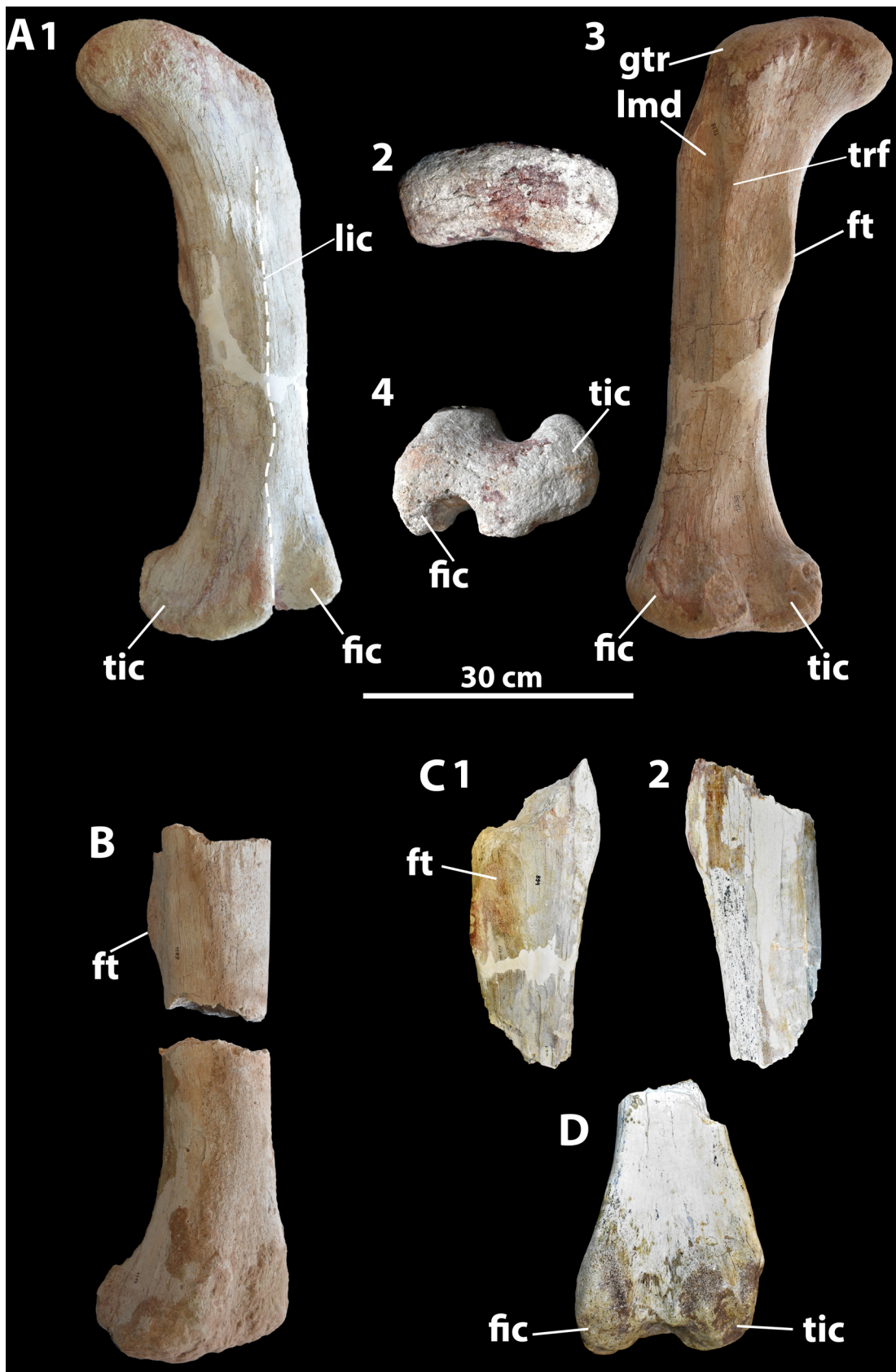


FIGURE 22. Femora of *Uberabatitan ribeiroi*. **A** CPPLIP-1238 left element in 1, oblique (anterior/lateral), 2, proximal, 3, oblique (posterior/medial) and 4, distal views; **B** CPPLIP-1189 left element in oblique (anterior/lateral) view; **C** CPPLIP-894 right element in 1, anterior and 2, posterior views; **D** CPPLIP-898 left element in anterior view. Abbreviations: **fic**: fibular condyle; **ft**: fourth trochanter; **gtr**: great trochanter; **lmd**: lateromedial depression; **lic**: linea intermuscularis cranialis; **tic**: tibial condyle; **trf**: trochanteric shelf.



FIGURE 23. Crural elements of *Uberabatitan ribeiroi*. **A** CPPLIP-917 (redefined holotype) left tibia in 1, lateral, 2, medial, 3, proximal and 4, distal views; **B** CPPLIP-1107 (redefined holotype) left fibula in 1, lateral, 2, medial, 3, proximal and 4, distal views; **C** CPPLIP-1106 left fibula in 1, lateral, 2, medial and 3, distal views; **D** CPPLIP-917 and CPPLIP-1107 (redefined holotype) articulated left tibia and fibula in 1, posterior and 2, anterior views. Abbreviations: **aa**: astragalar articulation; **cc**: cnemial crest; **fk**: fibular knob; **fvl**: fovea ligamentosa; **jc**: joint capsule; **M. fdl**: M. flexor digitorum longus; **M. il**: insertion for the M. iliofibularis; **lt**: lateral trochanter; **or**: oblique ridge; **prc**: proximal crest, **tp**: tibial protuberance.

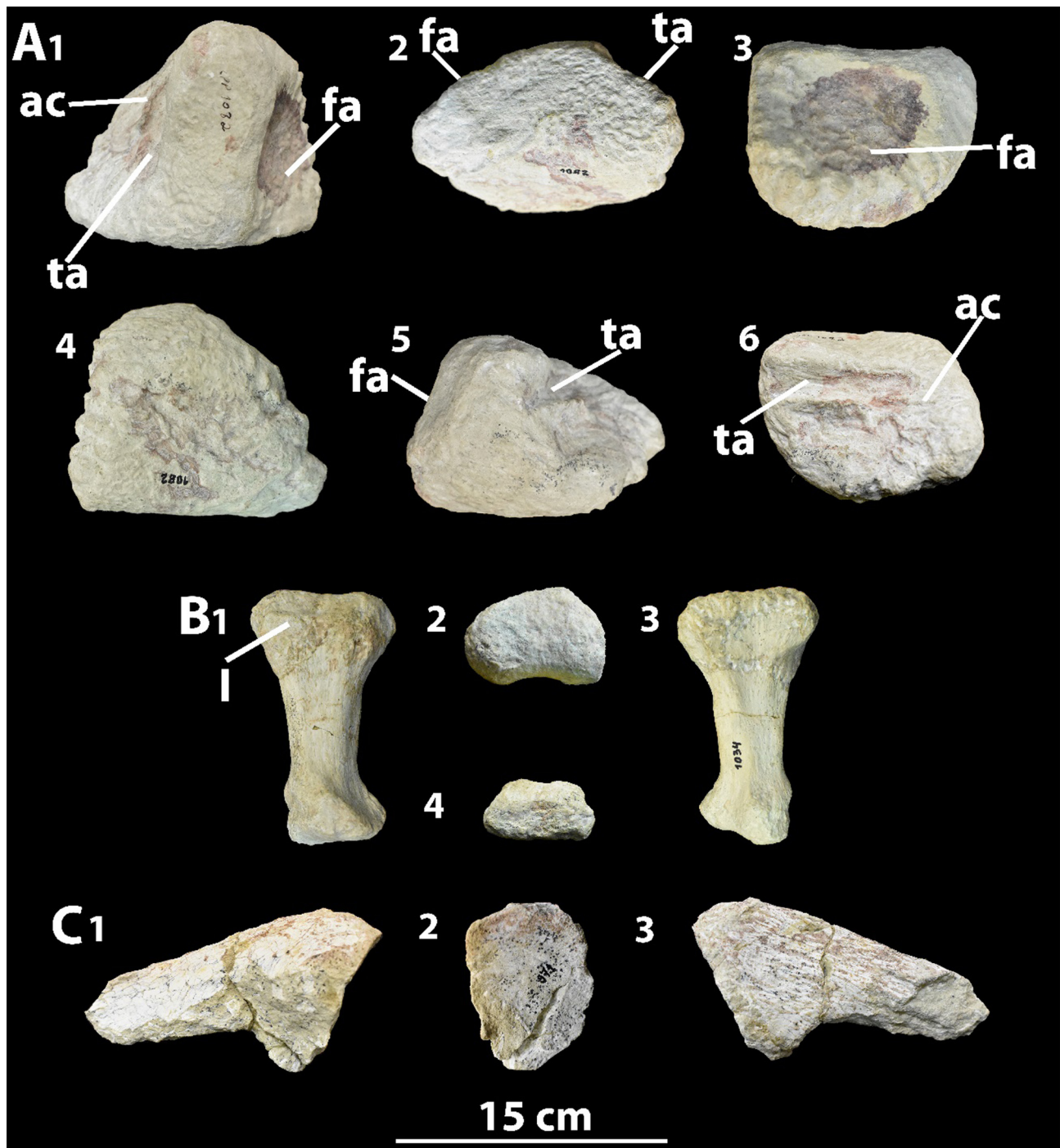
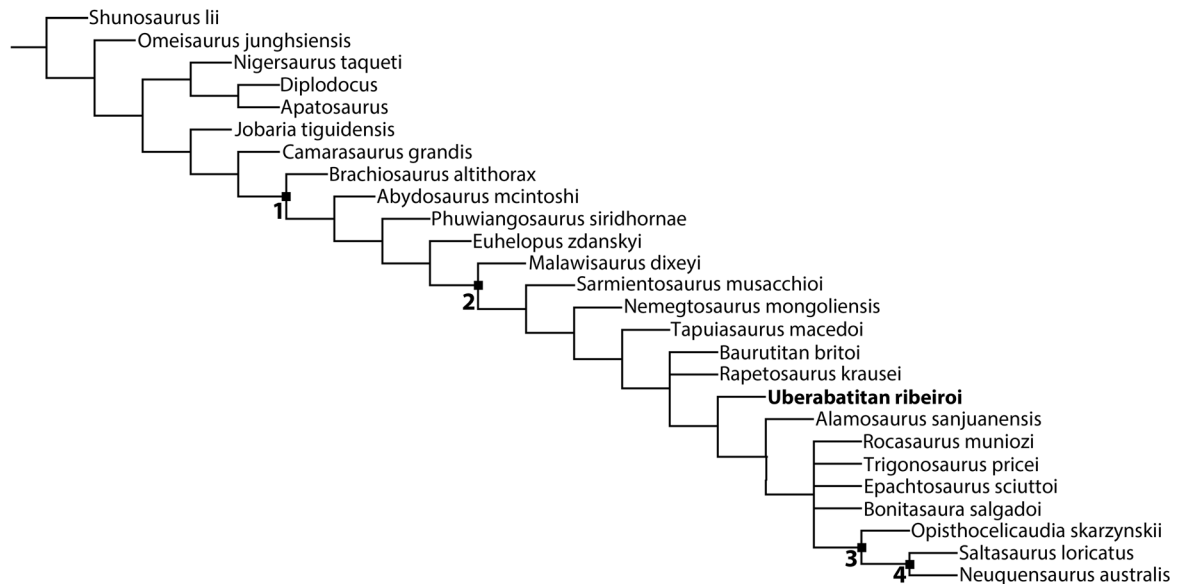


FIGURE 24. Pedal elements of *Uberabatitan ribeiroi*. **A** CPPLIP-1082 (redefined holotype) left astragalus in 1, proximal, 2, anterior, 3, lateral, 4, distal, 5, posterior, 6, medial views; **B** CPPLIP-1034 metatarsal II in 1, dorsal, 2, proximal, 3, plantar and 4, distal views and **C** CPPLIP-971 ungual phalanx in 1, lateral, 2, posterior and 3, medial views. Abbreviations: **I**: articulation with metacarpal I; **ac**: anteroposterior crest; **fa**: fibular articulation; **ta**: tibial articulation.

The analysis of the Martínez *et al.* (2016) dataset including *Uberabatitan* resulted in eight most parsimonious trees of 627 steps ($Ci=0.555$, $Ri=0.655$), the strict consensus of which shows *Uberabatitan* positioned as a non-Saltasauridae titanosaur (Fig. 25). As for the González Riga *et al.* (2018) dataset, apart from the addition of *Uberabatitan* and aiming at a more concise analysis, all species recovered as non-Titanosauriformes in the original study were excluded, with *Galveosaurus* Sanchez-Hernandez, 2005, kept as the outgroup. The result was 108 most parsimonious trees of 1169 steps ($Ci: 0.549$, $Ri: 0.770$), the strict consensus of which shows *Uberabatitan* as a non-Saltasauridae lithostrotian titanosaur (Fig. 26).

TABLE 11. Phylogenetic definitions of clade names used in this study.

Aeolosaurini Franco-Rosas <i>et al.</i> , 2004	Most inclusive clade including <i>Aeolosaurus rionegrinus</i> Powell, 1987a, and <i>Gondwanatitan faustoi</i> Kellner and Azevedo, 1999, but not <i>Saltasaurus loricatus</i> Powell, 1992
Brachiosauridae Riggs 1903 (sensu Wilson and Sereno, 1998)	Most inclusive clade including <i>Brachiosaurus altithorax</i> Riggs, 1903, but not <i>Saltasaurus loricatus</i> Bonaparte and Powell, 1980
Lithostrotia Wilson and Upchurch, 2003 (sensu Upchurch <i>et al.</i> , 2004)	Minimal clade including <i>Malawisaurus dixeyi</i> Jacobs <i>et al.</i> 1993 and <i>Saltasaurus loricatus</i> Bonaparte and Powell, 1980
Lognkosauria Calvo <i>et al.</i> , 2007a	Minimal clade including <i>Mendozasaurus neguyelap</i> González Riga, 2003, and <i>Futalognkosaurus dukei</i> Calvo <i>et al.</i> , 2007a
Rinconsauria Calvo <i>et al.</i> , 2007b	Minimal clade including <i>Muyelensaurus pecheni</i> Calvo, González Riga and Porfiri, 2007, and <i>Rinconsaurus caudamirus</i> Calvo and González Riga, 2003
Saltasauridae Bonaparte and Powell, 1980 (sensu Sereno 1998)	Minimal clade including <i>Ophistocelicaudia skarzynskii</i> Borsuk-Bialynicka 1977 and <i>Saltasaurus loricatus</i> Bonaparte and Powell, 1980
Saltasaurinae Powell 1986 (sensu Powell, 1992)	Minimal clade including <i>Neuquensaurus australis</i> Lydekker, 1883, and <i>Saltasaurus loricatus</i> Bonaparte and Powell 1980
Somphospondyli Wilson and Sereno 1998 (sensu Upchurch <i>et al.</i> , 2004; Mannion <i>et al.</i> , 2013)	Most inclusive clade including <i>Saltasaurus loricatus</i> Bonaparte and Powell 1980 but not <i>Brachiosaurus brancai</i> Janensch 1914
Titanosauria Bonaparte and Coria 1993 (sensu Wilson and Upchurch 2003)	Minimal clade including <i>Andesaurus delgadoi</i> Calvo and Bonaparte 1991 and <i>Saltasaurus loricatus</i> Bonaparte and Powell 1980
Titanosauriformes Salgado <i>et al.</i> 1997	Minimal clade including <i>Brachiosaurus altithorax</i> Riggs 1903 and <i>Saltasaurus loricatus</i> Bonaparte and Powell 1980

**FIGURE 25.** Strict consensus of 8 MPTs, based on Martínez *et al.* (2016). Nodes: 1—Titanosauriformes, 2—Lithostrotia/Somphospondyli, 3—Saltasauridae, 4—Saltasaurinae.

The results of both analyses agree that *Uberabatitan* represents a non-Saltasauridae “lithostrotian” titanosaur, similar to its positioning in the Gallina and Otero (2015) study, where *Uberabatitan* was found as a non-saltasaurine titanosaur. The position of *Uberabatitan* as a non-Saltasauridae is highly incongruent with that presented by Bandeira *et al.* (2016), where the species was recovered as the sister-taxon of *Brasilotitan* within Saltasaurinae. In order to test if new scorings and specimens could change those results, *Uberabatitan* was rescored on this dataset, with the change of seveten characters states and the addition of eight not previously coded (Appendix 3). As the authors did not inform the search parameters, we used those of Martínez *et al.* (2016). The

result was 26 most parsimonious trees of 228 steps (Ci: 0.249; Ri: 0.574). The strict consensus shows a polytomy with most taxa within Lithostrotia, whereas the 50% majority-rule consensus tree (Fig. 27) shows a topology similar to that recovered in the original authors but with *Uberabatitan* and *Brasilotitan* in a polytomy within Aeolosaurini. This result stresses the uncertainties related to Lithostrotia relationships, but reinforces the non-Saltasauridae position of *Uberabatitan*.

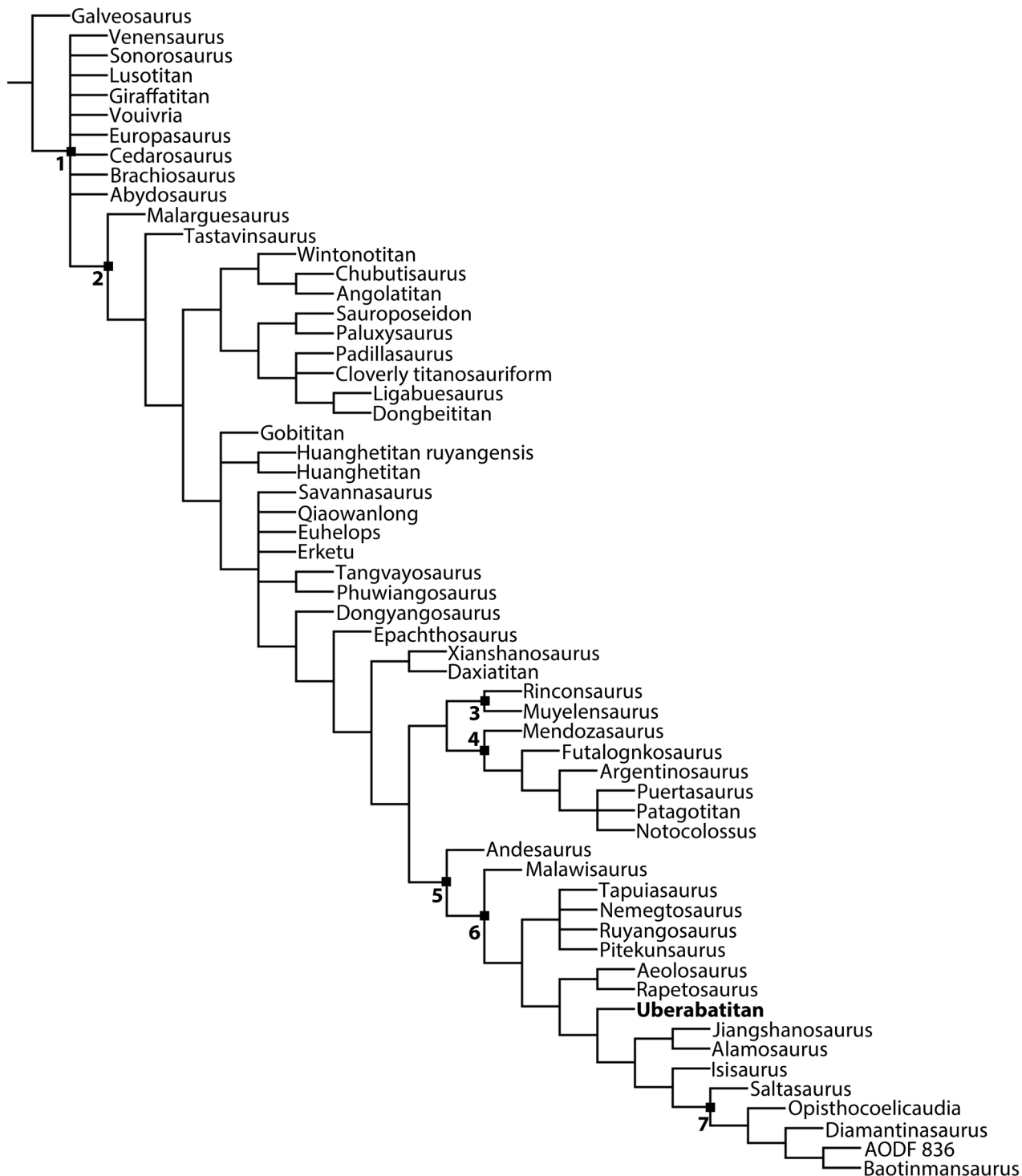


FIGURE 26. Strict consensus of 108 MPT, based on Gonzalez Riga *et al.* (2018). Nodes: 1—Titanosauriformes; 2—Somphospondyli; 3—Rinconsauria; 4—Lognkosauria; 5—Titanosauria; 6—Lithostrotia; 7—Saltasauridae.

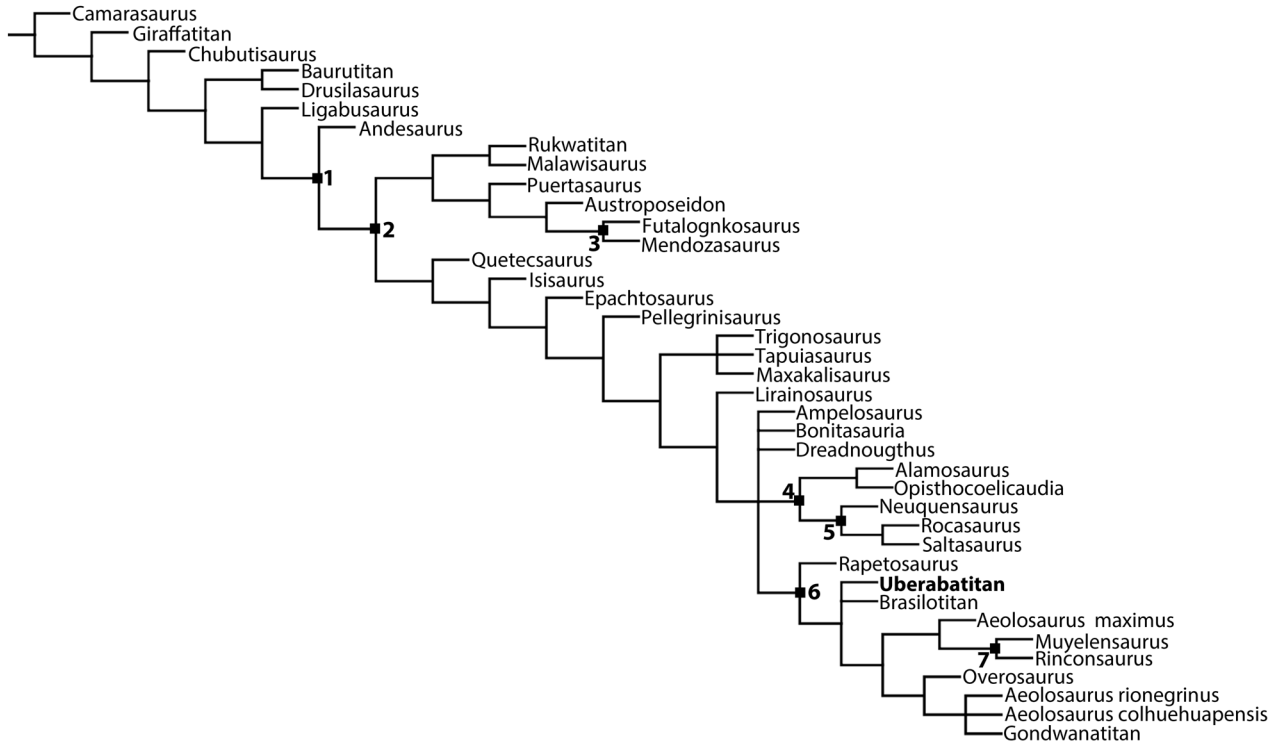


FIGURE 27. 50% majority-rule consensus of 26 MPT, based on Bandeira *et al.* (2017). Nodes: 1—Titanosauria; 2—Lithostrotia; 3—Lognkosauria; 4—Saltasauridae; 5—Saltasaurinae; 6—Aeolosaurini, 7—Rinconsauria.

COMPARISON TO OTHER BAURU GROUP TAXA

Apart from the phylogenetic uniqueness of *Uberabatitan* relative to the other Bauru Basin titanosaurs, as recognized in the performed analyses, the taxon also differs anatomically from all those taxa. The middle cervical vertebrae of *Uberabatitan* possess the neural spine lower than those of *Trigonosaurus* (MCT 1488-R, fig. 12) and *Maxakalisaurus* (MN 5013-V, fig. 7). The anterior and middle cervical vertebrae of *Uberabatitan* bear a ridge positioned on the ventrolateral part of the centrum that extends anteroposteriorly, a similar ridge is also seen in the anterior cervical vertebrae of *Trigonosaurus* (MCT 1488-R, fig. 6) and *Brasilotitan* (MPM 125R, fig. 5), but it is positioned strictly ventrally on the latter.

The anterior trunk vertebrae of *Uberabatitan* shows less pneumatization than those of *Austroposeidon* (MCT 1628-R, fig. 4A–B) and *Trigonosaurus* (MCT 1488-R, fig. 15), where the pleurocoels are deeper and divided on small fossae. The middle caudal vertebrae of *Uberabatitan* possess the concavity of its centra positioned in the center of the element, whereas those of *Maxakalisaurus* are more excavated anteriorly. Also, differing from *Adamantisaurus* (MUGEO 1282, figs. 1–8), the anterior and middle caudal vertebrae of *Uberabatitan* do not show any signs of pneumatization or foramina. As for the appendicular skeleton of *Uberabatitan*, the femur is significantly more robust than those of *Aeolosaurus maximus* (MPMA 12-0001-97, fig. 9A1–4), as is its humerus, compared to that of *Gondwanatitan* (MN 4111-V, fig. 20).

Finally, it is interesting to note the unusual pattern of the epiphysial-prezygapophyseal lamina present on the anterior and middle cervical vertebrae of *Uberabatitan*. This pattern can also be seen in the anterior cervical vertebrae of “DGM Series A” (MCT 1487-R; Powell, 1987b, 2003), also unearthed from the Serra da Galga Member, Marília Formation, from the site known as “Mumbuca” or Quarry 5 of the Serra do Veadinho Hill, near Peirópolis town (Campos and Kellner, 1999). This specimen was partially described by Powell (1987b, 2003) and briefly discussed by Wilson (2012), who recognized that the lamina located ventrally to its epiphysial-prezygapophyseal lamina corresponds to the zygapophyseal portion of the postzygodiapophyseal lamina. Yet, in the same papers, the author states that the only lamina that reaches the spinodiapophyseal fossa is the epiphysial-prezygapophyseal lamina. Therefore, the lamina of “DGM Series A” that reaches the ventral portion of the

spinodiapophyseal fossa, cannot be the postzygodiapophyseal lamina, but a zygapophyseal portion of the epiphysial-prezygapophyseal lamina. As such, it has the same configuration seen in *Uberabatitan*. Besides that feature, “DGM Series A” also shares with *Uberabatitan* anterior cervical vertebrae a ventrolateral ridge on the centrum and a “bulbous” (mediolaterally expanded) apex of the neural spine (Fig. 28). Based on these anatomical similarities and the same stratigraphic provenance, “DGM Series A” can be considered as very closely related to *Uberabatitan*, or perhaps even an individual of that taxon.

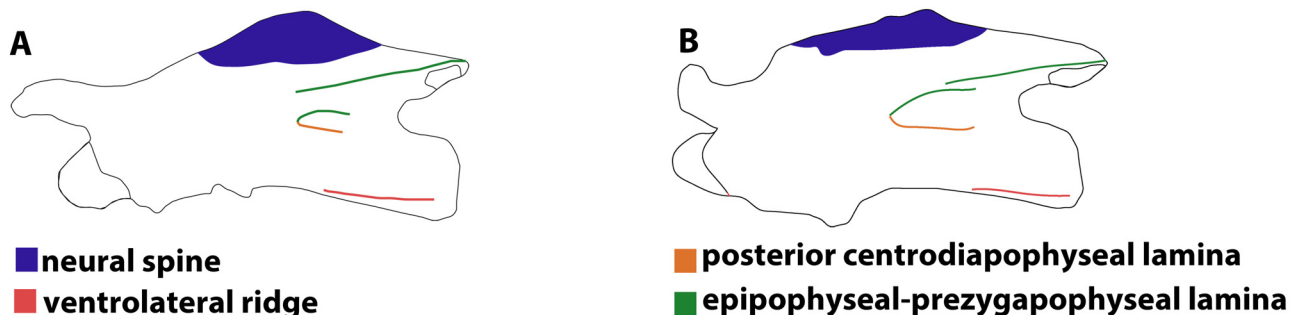


FIGURE 28. Interpretative drawn of anterior cervical vertebrae of **A** CPPLIP-1057 and **B** Serra do Veadinho “DGM Series A” (MCT 1487-R, 5th cervical), showing homologous structure between them.

Conclusions

A detailed description of all remains pertaining to *Uberabatitan*, with the attribution of new elements from the type-locality, allowed a better understanding of the taxon, with the identification of a new autapomorphy. A linear regression approach revealed that the bone assemblage of *Uberabatitan* is composed at least of five individuals with the presence of one juvenile and one giant specimen. Anatomic comparisons with “DGM Series A” indicate that this specimen is closely related or even can belong to *Uberabatitan*. Finally, a series of phylogenetic analyses recovered *Uberabatitan* as a non-Saltasauridae “lithostrotian” titanosaur, with possible close relationships to *Brasilotitan*.

Acknowledgements

We thank Luiz Carlos Borges Ribeiro and the staff of the Centro de Pesquisas Paleontológicas “Llewelyn Ivor Price” (UFTM) for field support, lab assistance and discussion. For access to collection we thank Rodrigo Machado (Museu de Ciências da Terra) and Luciana Barbosa (Museu Nacional). We thank John Fronimos and Pablo A. Gallina for review and criticism that greatly improved the strength of this paper. This work was supported by Conselho Nacional de Desenvolvimento Científico e Tecnológico (CNPq), Fundação de Amparo à Pesquisa do Estado de Minas Gerais (FAPEMIG) and Fundação de Amparo à Pesquisa do Estado de São Paulo (grant to M. C. L, process number 2014/03825-3).

References

- Bandeira, K.L., Simbras, F.M., Machado, E.B., de Almeida Campos, D., Oliveira, G.R. & Kellner, A.W. (2016) A new giant Titanosauria (Dinosauria: Sauropoda) from the Late Cretaceous Bauru Group, Brazil. *PLoS ONE*, 11 (10), e0163373. <https://doi.org/10.1371/journal.pone.0163373>
- Bittencourt, J.S. & Langer, M.C. (2011) Mesozoic dinosaurs from Brazil and their biogeographic implications. *Anais da Academia Brasileira de Ciências*, 83 (1), 23–60. <https://doi.org/10.1590/S0001-37652011000100003>
- Bonaparte, J.F., Heinrich, W.D. & Wild, R. (2000) Review of *Janenschia* Wild, with the description of a new sauropod from the Tendaguru beds of Tanzania and a discussion on the systematic value of procoelous caudal vertebrae in the sauropoda. *Palaeontographica Abteilung A*, 25–76.

- Borsuk-Bialynicka, M. (1977) A new camarasauroid sauropod *Opisthocoelicaudia skarzynskii* gen. n., sp. n. from the Upper Cretaceous of Mongolia. *Palaeontologia Polonica*, 37 (5), 5–64.
- Calvo, J.O. & Bonaparte, J.F. (1991) *Andesaurus delgadoi* gen. et sp. nov. (Saurischia-Sauropoda), dinosaurio Titanosauridae de la Formación Rio Limay (Albiano-Cenomaniano), Neuquén, Argentina. *Ameghiniana*, 28, 303–310.
- Calvo, J.O. & González Riga, B.J. (2003) *Rinconsaurus caudamirus* gen. et sp. nov., a new titanosauroid (Dinosauria, Sauropoda) from the Late Cretaceous of Patagonia, Argentina. *Revista geológica de Chile*, 30 (2), 333–353.
<https://doi.org/10.4067/S0716-02082003000200011>
- Calvo, J.O., Porfiri, J.D., González-Riga, B.J. & Kellner, A.W. (2007a) A new Cretaceous terrestrial ecosystem from Gondwana with the description of a new sauropod dinosaur. *Anais da Academia Brasileira de Ciências*, 79 (3), 529–541.
<https://doi.org/10.1590/S0001-37652007000300013>
- Calvo, J.O., González Riga, B.J. & Porfiri, J.D. (2007b) A new titanosauroid from the Late Cretaceous of Neuquén, Patagonia, Argentina. *Arquivos do Museu Nacional*, 65 (4), 485–504.
- Campos, D.D.A. & Kellner, A.W. (1999) On some sauropod (Titanosauridae) pelvises from the continental Cretaceous of Brazil. *National Science Museum Monographs*, 15, 143–166
- Campos, D.D.A., Kellner, A.W., Bertini, R.J. & Santucci, R.M. (2005) On a titanosauroid (Dinosauria, Sauropoda) vertebral column from the Bauru group, Late Cretaceous of Brazil. *Arquivos do Museu Nacional*, 63 (3), 565–593.
- Carballido, J.L., Pol, D., Cerda, I. & Salgado, L. (2011) The osteology of *Chubutisaurus insignis* del Corro, 1975 (Dinosauria: Neosauropoda) from the ‘middle’ Cretaceous of central Patagonia, Argentina. *Journal of Vertebrate Paleontology*, 31 (1), 93–110.
<https://doi.org/10.1080/02724634.2011.539651>
- Carballido, J.L. & Sander, P.M. (2013) Postcranial axial skeleton of *Europasaurus holgeri* (Dinosauria, Sauropoda) from the Upper Jurassic of Germany: implications for sauropod ontogeny and phylogenetic relationships of basal Macronaria. *Journal of Systematic Palaeontology*, 12 (3), 335–387.
<https://doi.org/10.1080/14772019.2013.764935>
- Coria, R.A., Filippi, L.S., Chiappe, L.M., Garcia, R. & Arcucci, A.B. (2013) *Overosaurus paradasorum* gen. et sp. nov., a new sauropod dinosaur (Titanosauria: Lithostrotia) from the Late Cretaceous of Neuquén, Patagonia, Argentina. *Zootaxa*, 3683 (4), 357–376.
<https://doi.org/10.11646/zootaxa.3683.4.2>
- Curry-Rogers, K. (2009) The postcranial osteology of *Rapetosaurus krausei* (Sauropoda: Titanosauria) from the Late Cretaceous of Madagascar. *Journal of Vertebrate Paleontology*, 29 (4), 1046–1086.
<https://doi.org/10.1671/039.029.0432>
- de Jesus Faria, C.C., Riga, B.G., dos Anjos Candeiro, C.R., da Silva Marinho, T., David, L.O., Simbras, F.M. & da Costa, P.V.L.G. (2015) Cretaceous sauropod diversity and taxonomic succession in South America. *Journal of South American Earth Sciences*, 61, 154–163.
<https://doi.org/10.1016/j.jsames.2014.11.008>
- Dias-Brito, D., Musacchio, E.A., de Castro, J.C., Maranhão, M.S.A.S., Suárez, J.M. & Rodrigues, R. (2001) Grupo Bauru: uma unidade continental do Cretáceo no Brasil-concepções baseadas em dados micropaleontológicos, isotópicos e estratigráficos. *Revue de Paléobiologie*, 20 (1), 245–304.
- Franco-Rosas, A.C., Salgado, L., Rosas, C.F. & Carvalho, I.D.S. (2004) Nuevos materiales de titanosauros (Sauropoda) en el Cretácico Superior de Mato Grosso, Brasil. *Revista Brasileira de Paleontología*, 7 (3), 329–336.
<https://doi.org/10.4072/rbp.2004.3.04>
- Gallina, P.A. & Otero, A. (2015) Reassessment of *Laplatasaurus araukanicus* (Sauropoda: Titanosauria) from the Upper Cretaceous of Patagonia, Argentina. *Ameghiniana*, 52 (5), 487–501.
<https://doi.org/10.5710/AMGH.08.06.2015.2911>
- Goloboff, P.A. & Catalano, S.A. (2016) TNT version 1.5, including a full implementation of phylogenetic morphometrics. *Cladistics*, 32 (3), 221–238.
<https://doi.org/10.1111/cla.12160>
- González Riga, B.J. (2003) A new titanosauroid (Dinosauria, Sauropoda) from the Upper Cretaceous of Mendoza province, Argentina. *Ameghiniana*, 40 (2), 155–172.
- González Riga, B.J. (2005) Nuevos restos fósiles de *Mendozasaurus neguyelap* (Sauropoda, Titanosauria) del Cretácico tardío de Mendoza, Argentina. *Ameghiniana*, 42 (3), 535–548.
- González Riga, B.J., Calvo, J.O. & Porfiri, J. (2008) An articulated titanosauroid from Patagonia (Argentina): new evidence of neosauropod pedal evolution. *Palaeoworld*, 17 (1), 33–40.
<https://doi.org/10.1016/j.palwor.2007.08.003>
- González Riga, B.J., Mannion, P.D., Poropat, S.F., David, O., Leonardo, D. & Coria, J. P. (2018) Osteology of the Late Cretaceous Argentinean sauropod dinosaur *Mendozasaurus neguyelap*: implications for basal titanosauroid relationships. *Zoological Journal of the Linnean Society*, 184 (1), 136–181.
<https://doi.org/10.1093/zoolinnean/zlx103>
- Gilmore, C.W. (1922) A new sauropod dinosaur from the Ojo Alamo formation of New Mexico. *Smithsonian Miscellaneous Collections*, 72 (14), 1–9.
- Jacobs, L., Winkler, D.A., Downs, W.R. & Gomani, E.M. (1993) New material of an Early Cretaceous titanosauroid from the Ojo Alamo formation, New Mexico. *Smithsonian Miscellaneous Collections*, 184 (14), 1–9.

- dinosaur from Malawi. *Palaeontology*, 36, 523–523.
- Janensch, W. (1914) Übersicht über die Wirbeltierfauna der Tendaguruschichten, nebst einer kurzer Charakterisierung der neu aufgeführten Arten von Sauropoden. *Archiv für Biologie*, 3, 81–110.
- Kellner, A.W. & Azevedo, S.D. (1999) A new sauropod dinosaur (Titanosauria) from the Late Cretaceous of Brazil. *National Science Museum Monographs*, 15, 111–142.
- Kellner, A.W.A., Campos, D.D.A. & Trotta, M.N. (2005) Description of a titanosaurid caudal series from the Bauru Group, Late Cretaceous of Brazil. *Arquivos do Museu Nacional*, 63 (3), 529–564.
- Kellner, A.W., Campos, D.D.A., Trotta, M.N., Azevedo, S.A.K., Craik, M.M. & Silva, H.P. (2006) On a new titanosaur sauropod from the Bauru Group, Late Cretaceous of Brazil. *Boletim do Museu Nacional, Geologia*, 74, 1–31.
- Lacovara, K.J., Lamanna, M.C., Ibíricu, L.M., Poole, J.C., Schroeter, E.R., Ullmann, P.V. & Egerton, V.M. (2014) A gigantic, exceptionally complete titanosaurian sauropod dinosaur from southern Patagonia, Argentina. *Scientific Reports*, 4, 6196. <https://doi.org/10.1038/srep06196>
- Lydekker, R. (1883) The dinosaurs of Patagonia. *Anales del Museo de la Plata* 2, 1–14.
- Machado, E.B., Avilla, L.S., Nava, W.R., Campos, D.A. & Kellner, A.W. (2013) A new titanosaur sauropod from the Late Cretaceous of Brazil. *Zootaxa*, 3701 (3), 301–321. <https://doi.org/10.11646/zootaxa.3701.3.1>
- Mannion, P.D., Upchurch, P., Barnes, R.N. & Mateus, O. (2013) Osteology of the Late Jurassic Portuguese sauropod dinosaur *Lusotitan atalaiensis* (Macronaria) and the evolutionary history of basal titanosauriforms. *Zoological Journal of the Linnean Society*, 168 (1), 98–206. <https://doi.org/10.1111/zoj.12029>
- Marsh, O.C. (1878) Principal characters of American Jurassic dinosaurs. *American Journal of Science*, 95, 411–416. <https://doi.org/10.2475/ajs.s3-16.95.411>
- Martin, V. (1994) Baby sauropods from the Sao Khua Formation (Lower Cretaceous) in northeastern Thailand. *Gaia*, 10, 147–153.
- Martinelli, A.G. & Teixeira, V.P.A. (2015) The Late Cretaceous vertebrate record from the Bauru Group at the Triângulo Mineiro, southeastern Brazil. *Boletín Geológico y Minero de España*, 126 (1), 129–158.
- Martinelli, A.G., Teixeira, V.P.A., Marinho, T.S., Fonseca, P.H., Cavallani, C.L., Araujo, A.J.G., Ribeiro, L.C.B. & Ferraz, M.L.F. (2015) Fused mid-caudal vertebrae in the titanosaur Uberabatitan ribeiroi (Dinosauria) from the Late Cretaceous of Brazil and other bone lesions. *Lethaia*, 48 (4), 429–560. <https://doi.org/10.1111/let.12117>
- Martínez, R.D., Lamanna, M.C., Novas, F.E., Ridgely, R.C., Casal, G.A., Martínez, J. E. & Witmer, L.M. (2016) A basal lithostrotian titanosaur (Dinosauria: Sauropoda) with a complete skull: implications for the evolution and paleobiology of Titanosauria. *PloS one*, 11 (4), e0151661. <https://doi.org/10.1371/journal.pone.0151661>
- Otero, A. (2010) The appendicular skeleton of *Neuquensaurus*, a Late Cretaceous saltasaurine sauropod from Patagonia, Argentina. *Acta Palaeontologica Polonica*, 55 (3), 399–426. <https://doi.org/10.4202/app.2009.0099>
- Otero, A. & Vizcaino, S.F. (2008) Hindlimb musculature and function of *Neuquensaurus australis* (Sauropoda: Titanosauria). *Ameghiniana*, 45 (2), 333–348.
- Owen, R. (1842) Report on British fossil reptiles. Part II. Report for the British Association for the Advancement of Science, Plymouth, 84, 60–294.
- Powell, J.E. (1986) *Revisión de los titanosáuridos de América del Sur*. Doctoral dissertation, Universidad Nacional de Tucumán, San Miguel de Tucumán, 340 pp.
- Powell, J.E. (1987a) The Late Cretaceous fauna from Los Alamitos, Patagonia, Argentina. Part. VI. The titanosaurids. *Revista Museo Argentino Ciencias Naturales*, 3 (3) 147–153.
- Powell, J.E. (1987b) Morfología del esqueleto axial de los dinosaurios titanosauridos (Saurischia, Sauropoda) del Estado de Minas Gerais. Brasil. *Anais Congresso Brasileiro de Paleontologia*, 101, 155–171.
- Powell, J.E. (1990) *Epachthosaurus sciuttoi* (gen. et sp. nov.) un dinosaurio saurópodo del Cretácico de Patagonia (Provincia de Chubut, Argentina). In: Congreso Argentino de Paleontología y Bioestratigrafía, Tucumán. Actas, 1, pp. 123–128).
- Powell, J.E. (1992) Osteología de *Saltasaurus loricatus* (Sauropoda-Titanosauridae) del Cretácico Superior del norte argentino. *Los Dinosaurios y su Entorno Biótico*, 165–230.
- Powell, J.E. (2003) *Revision of South American titanosaurid dinosaurs: palaeobiological, palaeobiogeographical and phylogenetic aspects*. Queen Victoria Museum and Art Gallery, Launceston, Tasmania, 173 pp.
- Price, L.I. (1951) Ovo de dinossauro na formação Bauru, do estado de Minas Gerais. *Notas Preliminares da Divisão de Geologia de Mineralogia*, 53, 1–7.
- Riggs, E.S. (1903) *Brachiosaurus altithorax*, the largest known Dinosaur. *American Journal of Science*, 15 (88), 299. [1880–1910] <https://doi.org/10.2475/ajs.s4-15.88.299>
- Riggs, E.S. (1904) *Structure and relationships of opisthocoelian dinosaurs: the Brachiosauridae*. Field Columbian Museum, Chicago, 28 pp.
- Salgado, L., Coria, R.A. & Calvo, J.O. (1997) Evolution of titanosaurid sauropods: Phylogenetic analysis based on the

- postcranial evidence. *Ameghiniana*, 34 (1), 3–32.
- Salgado, L. & Carvalho, I.S. (2008) *Uberabatitan ribeiroi*, a new titanosaur from the Marília Formation (Bauru group, Upper Cretaceous), Minas Gerais, Brazil. *Palaeontology*, 51 (4), 881–901.
<https://doi.org/10.1111/j.1475-4983.2008.00781.x>
- Salgado, L. & García, R. (2002) Variación morfológica en la secuencia de vértebras caudales de algunos saurópodos titanosauros. *Revista Española de Paleontología*, 17 (2), 211–216.
- Sanchez-Hernandez, B. (2005) *Galveosaurus herreroi*, a new sauropod dinosaur from Villar del Arzobispo Formation (Tithonian-Berriasian) of Spain. *Zootaxa*, 1034 (1), 1–20.
<https://doi.org/10.11646/zootaxa.1034.1.1>
- Santucci, R.M. & Arruda-Campos, A.C. (2011) A new sauropod (Macronaria, Titanosauria) from the Adamantina Formation, Bauru Group, Upper Cretaceous of Brazil and the phylogenetic relationships of Aeolosaurini. *Zootaxa*, 3085, 1–33.
- Santucci, R.M. & Bertini, R.J. (2006) A new titanosaur from western São Paulo state, upper Cretaceous Bauru Group, south-east Brazil. *Palaeontology*, 49 (1), 59–66.
<https://doi.org/10.1111/j.1475-4983.2005.00527.x>
- Seeley, H.G. (1888) Classification of the Dinosauria. *Geological Magazine*, 5 (1), 45–46.
<https://doi.org/10.1017/S0016756800156006>
- Sereno, P.C. (1998) A rationale for phylogenetic definitions, with application to the higher-level taxonomy of Dinosauria. *Neues Jahrbuch für Geologie und Paläontologie, Abhandlungen*, 210 (1), 41–83.
<https://doi.org/10.1127/njgpa/210/1998/41>
- Team, R. (2013) R development core team. *RA Lang Environ Stat Comput*, 55, 275–286.
- Tykoski, R.S. & Fiorillo, A.R. (2017) An articulated cervical series of *Alamosaurus sanjuanensis* Gilmore, 1922 (Dinosauria, Sauropoda) from Texas: new perspective on the relationships of North America's last giant sauropod. *Journal of Systematic Palaeontology*, 15 (5), 339–364.
<https://doi.org/10.1080/14772019.2016.1183150>
- Upchurch, P., Barret, P.M. & Dodson, P. (2004) Sauropoda. In: Weishampel, D.B., Dodson, P. & Osmólska, H. (Eds.), *The Dinosauria. 2nd Edition*. University of California Press, Berkeley, pp. 259–322.
<https://doi.org/10.1525/california/9780520242098.003.0015>
- Wilson, J. (2002) Sauropod dinosaur phylogeny: critique and cladistic analysis. *Zoological Journal of the Linnean Society*, 136 (2), 215–275.
<https://doi.org/10.1046/j.1096-3642.2002.00029.x>
- Wilson, J.A. (2006) An overview of titanosaur evolution and phylogeny. Actas de las III In: *Jornadas sobre Dinosaurios y su Entorno Biótico*. Salas de los Infantes, Burgos, pp. 169–190.
- Wilson, J.A. (2012) New vertebral laminae and patterns of serial variation in vertebral laminae of sauropod dinosaurs. *Contributions from the Museum of Paleontology, University of Michigan*, 32 (7), 91–110
- Wilson, J.A. & Sereno, P.C. (1998) Early evolution and higher-level phylogeny of sauropod dinosaurs. *Journal of Vertebrate Paleontology*, 18 (Supplement 2), 1–79.
- Wilson, J.A. & Carrano, M.T. (1999) Titanosaurs and the origin of “wide-gauge” trackways: a biomechanical and systematic perspective on sauropod locomotion. *Paleobiology*, 25 (2), 252–267.
<https://doi.org/10.1017/S0094837300026543>
- Wilson, J.A. & Upchurch, P. (2003) A revision of *Titanosaurus* Lydekker (dinosauria?sauropoda), the first dinosaur genus with a ‘Gondwanan’ distribution. *Journal of Systematic Palaeontology*, 1 (3), 125–160.
<https://doi.org/10.1017/S1477201903001044>
- Wilson, J.A., D'emic, D.M., Ikejiri, T., Moacdieh, E.M. & Whitlock, J.A. (2011) A nomenclature for vertebral fossae in sauropods and other saurischian dinosaurs. *PLoS ONE*, 6 (2), e17114.
<https://doi.org/10.1371/journal.pone.0017114>
- Wiman, C. (1929) Die Kreide-Dinosaurier aus Shantung. *Palaeontologia Sinica*, Series C, 6, 1–67.
- Zaher, H., Pol, D., Carvalho, A.B., Nascimento, P.M., Riccomini, C., Larson, P. & de Almeida Campos, D. (2011) A complete skull of an Early Cretaceous sauropod and the evolution of advanced titanosaurs. *PLoS One*, 6 (2), e16663.
<https://doi.org/10.1371/journal.pone.0016663>

APPENDIX 1. Coding for the data matrix of Martinez *et al.* (2016)

??1??11201
 00?1000?0?0?110000?01010100?????????????0?????0?????0?????2000101100?100010001110?01?1?1?01????????????
 ??1??2011?0?111?????????01?1??111?????????????????????1??10101112011101111110121111110????????1?????????
 ??????

APPENDIX 2. Coding for the data matrix of Bandeira *et al.* (2016)

?????????????????????????110100??10?1110100????100?1?3{01}?01101100??1?1???1?????11??000

APPENDIX 3. Characters changed from Bandeira *et al.* (2016)

Character number	Bandeira <i>et al.</i> (2016)	This study
29	1	0
31	1	?
32	0	?
34	1	0
35	1	?
38	?	1
40	1	0
42	1	0
44	1	?
45	1	?
46	1	?
48	0	?
49	0	1
51	1	0
53	?	1
54	1	?
55	0	3
56	?	0/1
62	0	1
65	?	1
66	1	?
68	?	1
74	?	1
81	?	1
82	?	1

APPENDIX 4. Coding for the data matrix of Gonzalez Riga *et al.* (2018)

?????????????0?0?0??10210110000?????????00101?????????????1011111?????????????????????????????????????
 ?????1000000?0-1000-?001-1??1011?????00????100?????0?11?0?0?0-0100??11-
 00?110000001??02??0011?????????211?11?????11?????1?????1?????11012101011?????????0??111?????????????
 ??????????????????100100?100??01?????????0101??00????000??1??0?????????1??011??11?????00001
 ?0000??0??0????